ELSEVIER

Precambrian Research 117 (2002) 269–294

Precambrian Research

www.elsevier.com/locate/precamres

Griffin gabbro sills (2.11 Ga), Hurwitz Basin, Nunavut, Canada: long-distance lateral transport of magmas in western Churchill Province crust

Lawrence B. Aspler [a,*], Brian L. Cousens [b], Jeffrey R. Chiarenzelli [c]

[a] *23 Newton Street, Ottawa, ON, Canada K1S 2S6*
[b] *Department of Earth Sciences, Carleton University, Ottawa, ON, Canada K1S 5B6*
[c] *Department of Geology, State University of New York at Potsdam, Potsdam, NY 13676, USA*

Received 31 July 2001; accepted 28 June 2002

Abstract

Circa 2.11 Ga sills and rare dykes (herein named the 'Griffin gabbros') extend discontinuously across an area 400 by 125 km in the Hearne domain of the western Churchill Province in northern Canada. Sills form poorly connected, tongue-like tabular bodies primarily within Paleoproterozoic intracratonic basin deposits of the lower Hurwitz Group. Dykes are restricted to the southern limit of the Griffin suite and have not been found in the interior of Hurwitz Basin or in Archean basement. Incompatible element patterns and low ε_{Nd}^{2111} values (-0.1 – $+1.0$) indicate an enriched asthenosphere source. Similar to many modern hotspot-related ocean island basalts, the gabbros display enrichments in Nb and La, suggesting a mantle plume origin. Heavy rare earth element depletions and TiO_2 values (averaging 3.40 wt.%) suggest partial melting of a garnet peridotite source at depths of 70–100 km; MgO values (averaging 5.20 wt.%) indicate fractionation after melting. Concentrations of both the incompatible and compatible elements scatter widely with respect to Mg number, indicating that compositional variation does not represent fractional crystallization from a common parent, consistent with derivation from different magma chambers related to the same mantle plume. The gabbros fail to show signs of an Archean enrichment event recorded by other Paleoproterozoic mafic rocks in the Hearne domain. This, together with the absence feeder dykes in basement, indicate derivation external to Hurwitz Basin. We interpret that a mantle plume, located beyond the present southern margin of the Hearne domain, was active during $\sim$2.1 Ga rifting that led to opening of the Manikewan ocean. The Griffin gabbros were likely injected because of the hydraulic head created by topographic doming above this plume. Analogous to the Ferrar sills (Jurassic) in Antarctica, the gabbros may have been fed by cryptic dykes in which magmas traveled laterally for at least 250 km across the southern Hearne domain and then, controlled by sedimentary layering, spread as sills for hundreds of km within Hurwitz Basin.

Keywords: Gabbro sills and dykes; Geochemistry; Hearne domain; Hurwitz Group; Sm–Nd isotopes; Magma transport

* Corresponding author
E-mail address: nwtgeol@sympatico.ca (L.B. Aspler).

0301-9268/02/$ - see front matter
PII: S0301-9268(02)00090-6

1. Introduction

Gabbro sills and dykes are significant components of continental flood basalt provinces that, relatively protected from removal by erosion, may be the only record of large-scale Precambrian volcanic events (Ernst and Buchan, 1997a). Commonly associated with mantle plumes, voluminous mafic magmatism on the continents is typically attributed to decompression melting of hot athenospheric mantle within plume heads, or decompression and conductive melting of lithospheric mantle above plume heads (White and McKenzie, 1995; Turner et al., 1996; Ernst and Buchan, 1997a,b, 2001a; Hawkesworth et al., 2000; Campbell, 2001; Condie, 2001). Although some would argue in favour of upwellings related to plate reorganizations and upper mantle convection cells (Anderson, 1998), recent seismic tomography has provided compelling images of discrete plumes, some of which extend upward from the core-mantle boundary (Zhao, 2001).

Work on giant dyke swarms has largely confirmed that mafic rocks need not be derived from immediately underlying mantle sources, and that magmas are capable of traveling laterally in the crust for hundreds to thousands of km away from plume centres (Fahrig, 1987; Greenough and Hodych, 1990; Ernst and Buchan, 1997a, 2001a,b; Ernst and Buchan, in press, Ernst et al., 2001). Large sills are also found at great distances from plume centres, but these are typically associated with laterally extensive dykes (Ernst and Buchan, 1997b, 2001a). Such dykes are generally considered the conduits through which long-distance lateral magma transport occurred, and to have either fed magma directly into sills or rolled over to become sills (Hyndman and Alt, 1987; White, 1992; Ernst and Buchan, 1997b, 2001a). Long-distance transport through subhorizontal pathways to form sills, considered theoretically by McKenzie et al. (1992), is not commonly recognized. A notable exception, the Ferrar sills in Antarctica (Jurassic) continue laterally for greater than 3000 km in the absence of significant feeder dykes in basement (Elliot et al., 1999).

The interval 2.2–2.0 Ga was a time of widespread global mafic magmatism. Dyke and sill swarms of this age, possibly related to the breakup of a speculative Neoarchean supercontinent ('Kenorland' of Williams et al., 1991), are found in Fennoscandia, Greenland, Siberia, and North America (Aspler and Chiarenzelli, 1998; Buchan et al., 1998, 2000; Ernst and Buchan, 2001b, and references therein). Forming part of this extensive suite, $\sim$2.11 Ga gabbro sills (and rare dykes), herein referred to as the 'Griffin gabbros', extend across an area of about 50 000 km^2 in the central Hearne domain of the western Churchill Province in northern Canada (Figs. 1 and 2). These sills occur primarily within Paleoproterozoic siliciclastic intracratonic basin strata of the lower Hurwitz Group (Figs. 3 and 4).

In the first part of this paper we describe the Griffin gabbro sills, documenting their distribution, geometric relationships to host rocks and rare dykes, contacts, internal structures, and regional geochemical and Sm–Nd isotopic characteristics. In the second part we consider the derivation of the sills and their emplacement mechanisms. Both field and geochemical data indicate that the Griffin gabbros originated outside of Hurwitz Basin, and that they constitute a Proterozoic example, analogous to the Ferrar sills, where mafic magmas travelled long distances laterally within the crust. We interpret that the gabbros were derived from a mantle plume beyond the present southern margin of the Hearne domain, and that this plume was active during $\sim$2.1 Ga rifting that led to opening of the Manikewan ocean (Stauffer, 1984), which separated the Hearne, Sask, and Superior cratons before collisional events in Trans-Hudson orogen (Fig. 1).

2. Geologic setting

The Griffin sills were emplaced at 2111 $\pm$ 1 Ma (Patterson and Heaman, 1991; Heaman and LeCheminant, 1993), after deposition of the lower part of the Hurwitz Group (sequences 1 and 2, Fig. 3). The Hurwitz Group is a succession of continental to marine siliciclastic and carbonate deposits that are distributed in a series of outliers across an area 200 by 700 km (Figs. 1 and 2). Sequences 1 and 2 record the evolution of an intracratonic basin that occupied

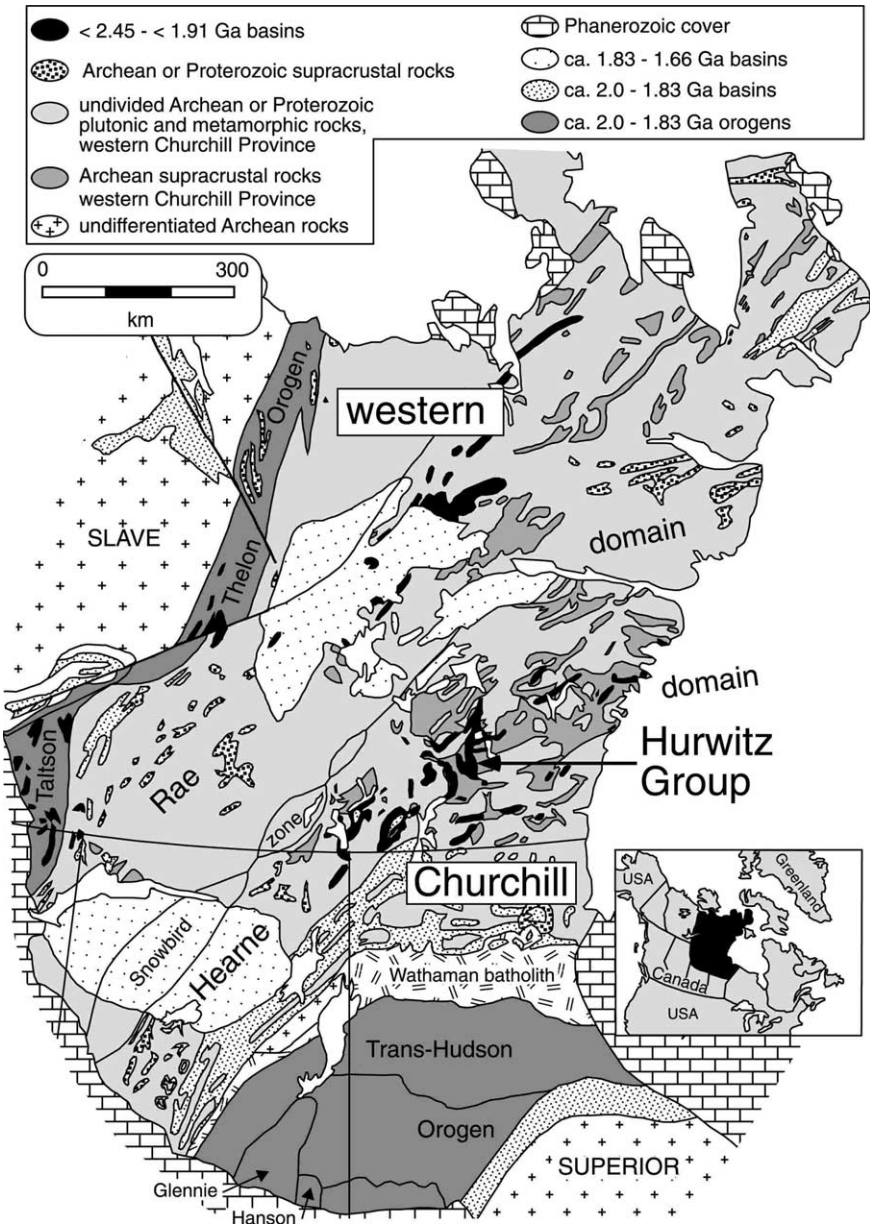

Fig. 1. Regional context of Hurwitz Basin and Griffin gabbro sills, Western Churchill Province. The Sask Craton (not outlined) is a basement terrane in the interior of Trans-Hudson orogen that extends southward beneath Phanerozoic cover from rare exposures in structural windows in the Glennie Lake and Hanson Lake domains (Chiarenzelli et al., 1998).

the interior of the Hearne domain during the breakup of Kenorland, whose daughter fragments ultimately dispersed at 2.1–2.0 Ga (Aspler and Chiarenzelli, 1998; Aspler et al., 2001). Deposition of upper Hurwitz Group strata (sequences 3 and 4, Fig. 3) overlapped, in part, with the assembly of Laurentia (Aspler et al., 2001; Aspler and Chiarenzelli, 2002).

The Hurwitz Group lies unconformably above an Archean basement that includes: ~3.3–3.0 Ga

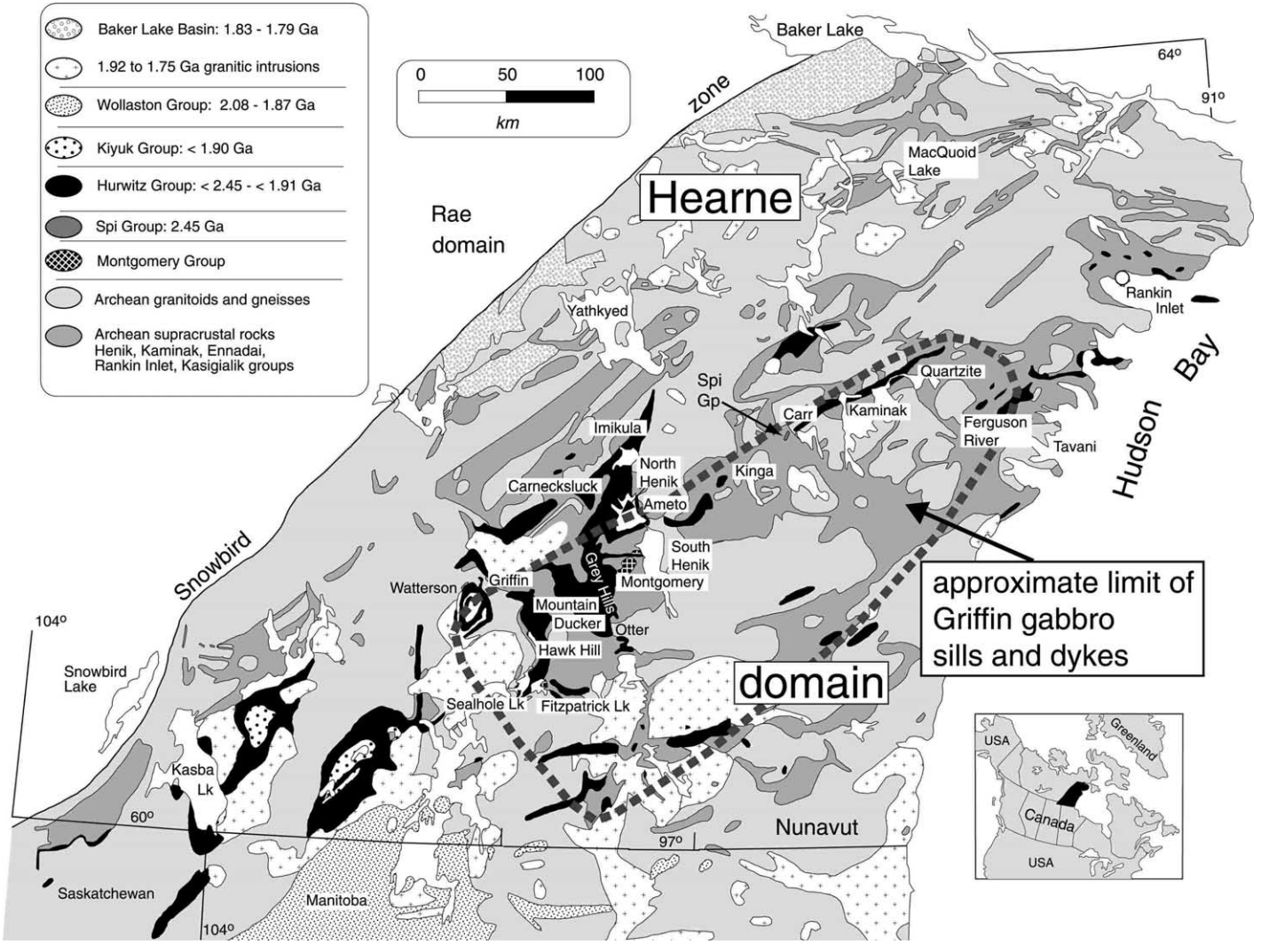

Fig. 2. Extent of the Griffin gabbros and simplified geology of the Hearne domain.

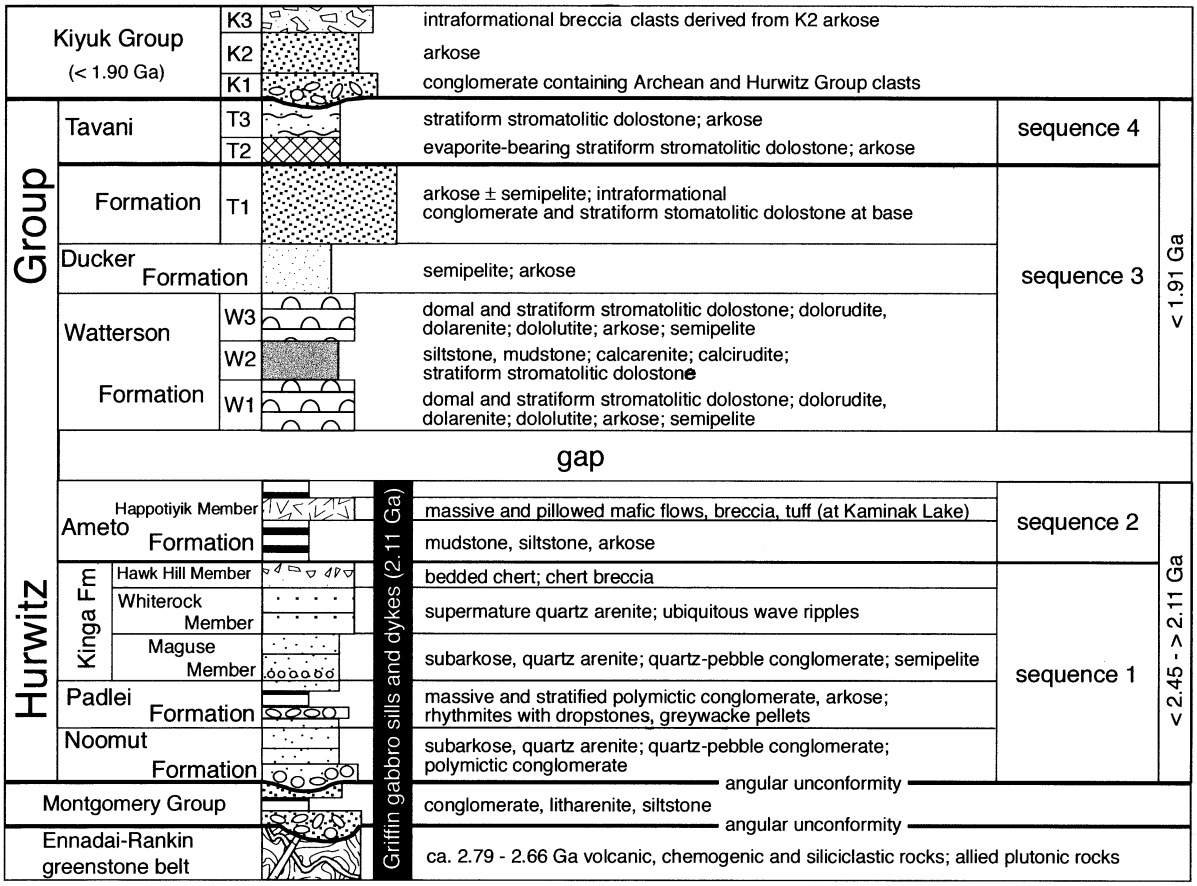

Fig. 3. Lithostratigraphy and sequence stratigraphy of the Hurwitz Group and stratigraphic context of the Griffin gabbros.

gneisses; ~2.79–2.66 Ga volcanic, siliciclastic and chemogenic rocks; and ~2.74–2.55 Ga plutonic and gneissic rocks (Aspler and Chiarenzelli, 1996a; Hanmer et al., 2000). Griffin sills and dykes are unknown within Archean basement. The Montgomery Group (Figs. 2 and 3) is a local, predominantly fluvial, siliciclastic wedge of uncertain age and tectonic significance that is separated from underlying Neoarchean supracrustal rocks and overlying Hurwitz Group strata by angular unconformities (Aspler and Chiarenzelli, 1996b; Aspler et al., 2000). At Fitzpatrick Lake (Fig. 4), the Montgomery Group is cut by Griffin gabbros.

A maximum age of Hurwitz Basin is defined by ~2.45 Ga baddeleyite (Heaman, 1994) from the Kaminak dykes, a laterally extensive mafic swarm that cuts basement rocks but not the Hurwitz Group. Mafic volcanic and siliciclastic rocks of the Spi Group (Patterson, 1991), likely extrusive equivalents to the Kaminak swarm (Beavon, 1976; Sandeman et al., 2000), separate Archean greenstones from the Hurwitz Group near Carr Lake (Fig. 2). Lacking direct geochronologic confirmation, the best estimate for the start of Hurwitz Basin sedimentation is ~2.3 Ga. This estimate is based on long-standing (Young, 1988) formation-level correlations of units in sequence 1 (Noomut, Padlei and Kinga formations, Fig. 3) with those at the top of the Huronian Supergroup (Cobalt Group) in the Superior craton. Predomi-

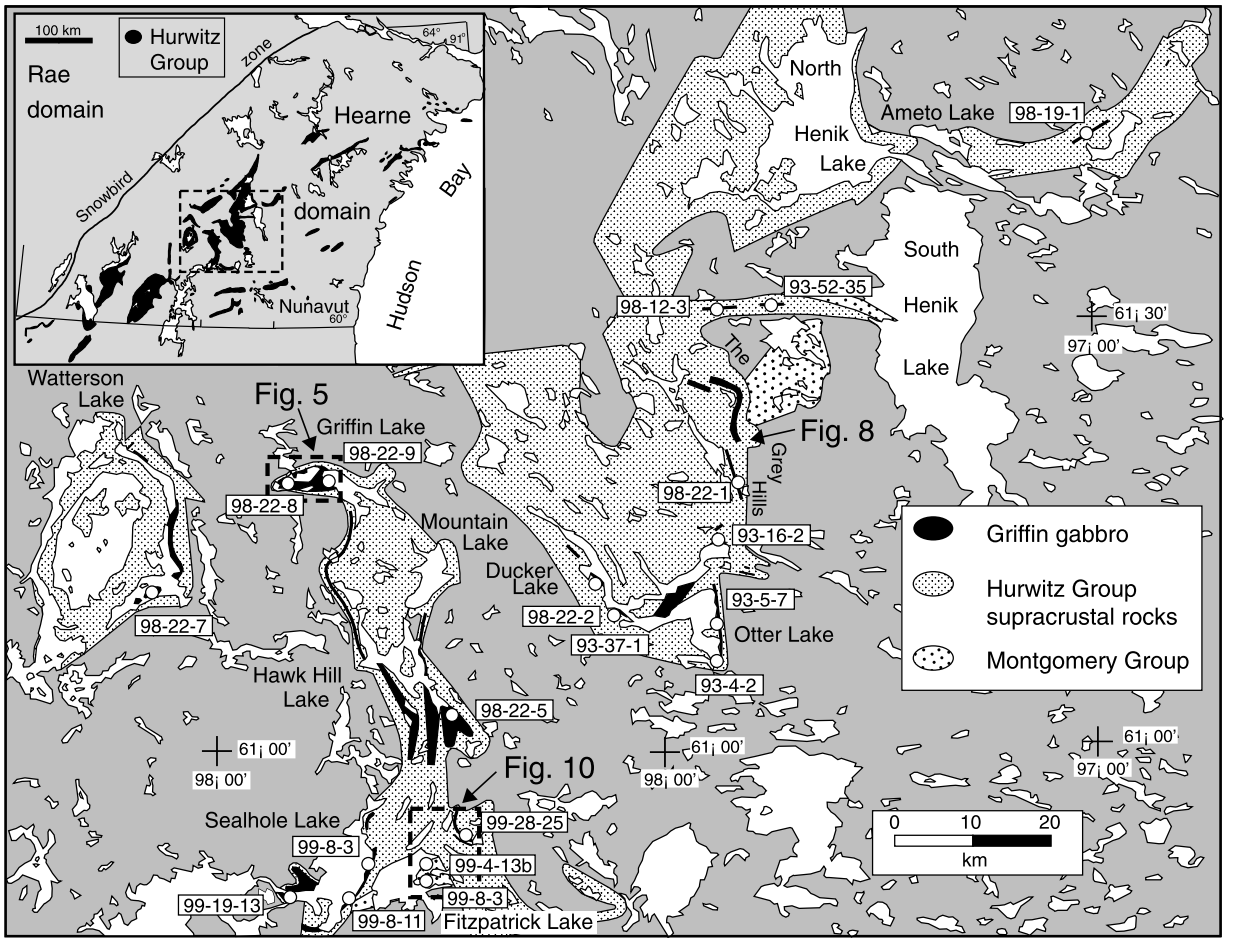

Fig. 4. Distribution of Griffin gabbros and sample sites, southern Hurwitz Basin.

nantly continental siliciclastic deposits of sequence 1 record development of a broad, shallow continental depression (Aspler et al., 2001). In sequence 2, immature pelites of the Ameto Formation, containing local mafic volcanic flows (Happotiyik Member, Fig. 3), reflect basin-margin arching and basin-centered deepening related to a second episode of stretching. The Griffin gabbros were emplaced after these initial stretching episodes, shortly before or during rift-passive margin sedimentation on the southern flank of the Hearne domain (lower Wollaston Group, Figs. 1 and 2; Yeo et al., 2000), which started before 2075 ± 2 Ma (Ansdell et al., 2000).

3. Griffin gabbros

3.1. Definition and distribution

Tabular gabbro sills occur in Hurwitz Group outliers across a wedge-shaped area 400 long and 125 km wide (Fig. 2). These intrusive rocks have conventionally been referred to as the 'Hurwitz gabbros'. Herein we introduce the term 'Griffin gabbros', to avoid confusion with gabbroic extrusive rocks that form part of the Happotiyik Member (Fig. 3). Particularly extensive exposures are in the type area at Griffin Lake, where sills define prominent ridges along the southern limb of

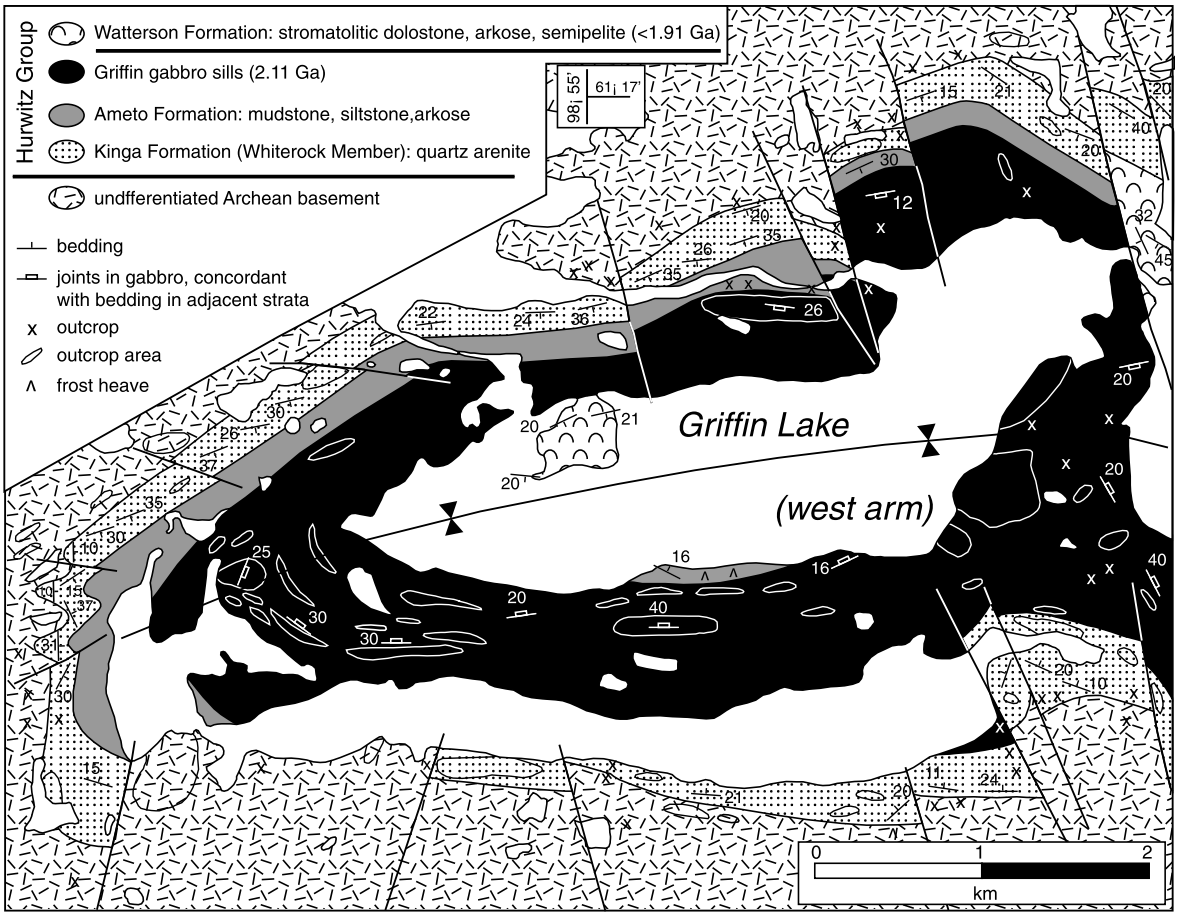

Fig. 5. Simplified geological map of the Griffin gabbro type area, west arm of Griffin Lake (modified after Aspler and Bursey, 1990). See Figs. 2 and 4 for location.

an east-plunging syncline (Figs. 4 and 5). The sills were folded together with Hurwitz Group sedimentary units under lower greenschist facies conditions as part of regional thick-skinned (Archean basement-Paleoproterozoic cover) deformation (Aspler et al., 2002). Paleomagnetic data from two sills with significantly different tilts indicate that the gabbros were remagnetized after folding (K.L. Buchan, unpublished data).

In other basins (Francis, 1982), sill and sediment rock isopachs coincide, and sills are thickest at sites of maximum sediment accumulation, forming bodies that are saucer-shaped at the regional-scale. However, as illustrated in Fig. 6, the Griffin sills fail to show a systematic relationship to Hurwitz Group depositional patterns. Successive units in sequence 1 onlap radially, spreading outward from a centre near the Henik lakes, and sequence 2 attains a maximum thickness near Ducker Lake and the northern part of The Grey Hills. The Griffin sills are scattered independent of this basin fill geometry: their thickness, number, and lateral continuity bear no relation to the centre of the basin.

The Griffin sills are generally less than a few hundred metres beneath the sub-sequence 3 unconformity and have no extrusive equivalents (see below). The possibility that volcanic rocks formed

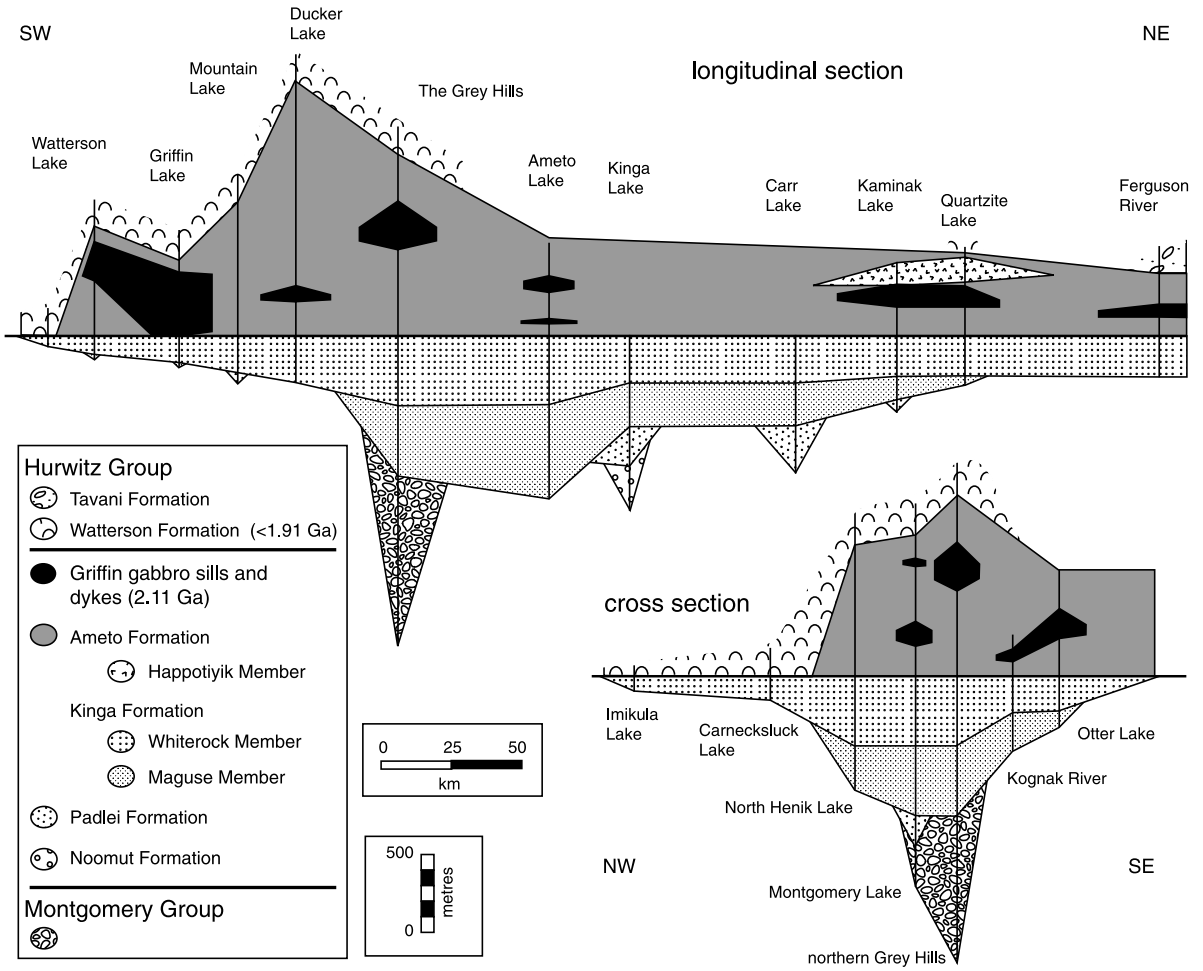

Fig. 6. Regional stratigraphic sections illustrating distribution of Griffin gabbro sills with respect to sedimentary fill of sequence 1 (Noomut, Padlei and Kinga formations) and sequence 2 (Ameto Formation). Sill number, thickness and continuity fail to coincide with radial sedimentation pattern displayed by sequence 1, and by sequence 2 depocentres. Section locations are given in Figs. 2 and 4 and plotted on a geographic base. Thicknesses are estimates based on map data. Sources: Watterson Lake, Aspler et al., (1993b); Griffin, Mountain and Hawk Hill lakes, Aspler and Bursey (1990); Ducker Lake, Otter Lake and Kognak River, Aspler et al. (1994); Montgomery Lake and The Grey Hills, Aspler et al. (1992); North Henik Lake, Aspler and Chiarenzelli (1997); Ameto and Kinga lakes Aspler et al. (1993a); Carr, Kaminak and Quartzite lakes (Bell, 1968; Hofmann and Davidson, 1998); Ferguson River, (Bell, 1968; Heywood, 1973); Imikula and Carnecksluck lakes (Eade, 1974).

coeval with the sills, but were eroded before deposition of sequence 3 cannot be dismissed entirely, given that emplacement depths of similar bodies elsewhere typically range from 1000 to 2500 m (Mudge, 1968), km-scale vertical uplifts may be associated with emplacement of sills (Gvirtzman and Garfunkel, 1997), and the time gap between Griffin magmatism and deposition of sequences 3 and 4 is at least 200 Ma (Davis et al., 2000).

3.2. Sill geometry

The Griffin sills are tongue-like, tabular bodies that are concordant with (or gently inclined to) bedding in enclosing strata. They generally occur in thinly stratified pelites of the Ameto Formation, well within the Ameto section. But at Griffin Lake and southwestern Sealhole Lake, they follow the Whiterock Member-Ameto Formation contact

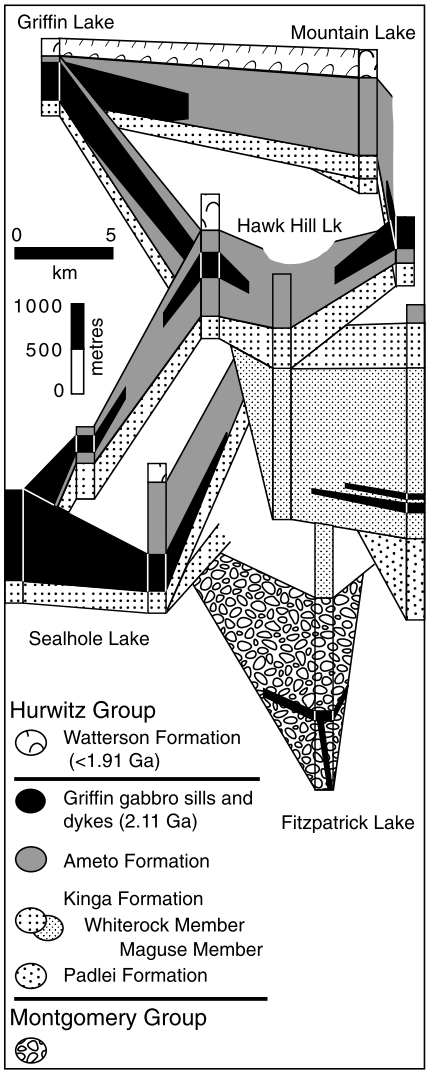

Fig. 7. Fence diagram, Griffin Lake to Fitzpatrick Lake. Note discontinuous nature of sills, and feeder dykes cutting Montgomery Group and Maguse Member at Fitzpatrick Lake. Based on 1:50 000-scale mapping (Aspler and Bursey, 1990; Aspler et al., 2000). See Figs. 2 and 4 for location.

(Fig. 7). In addition, sills with similar field, petrographic and geochemical characteristics are locally found in underlying units: at Fitzpatrick Lake they cut conglomeratic arkoses of the Montgomery Group and subarkoses of the Maguse Member (Fig. 7; Aspler et al., 2000), and at Quartzite Lake (Fig. 2), they cut quartz arenites of the Whiterock Member (Bell, 1968). They typically have thicknesses of 50–300 m (Figs. 6–8). The thickest sill (up to 1000 m) is at Sealhole Lake; it contains abundant plagioclase megacrysts and displays well-developed magmatic layering (see below). Recognized previously by Eade (1974), some of the thicker sills are composite intrusions, as indicated by local sill-in-sill chilled margins.

In two dimensional slices, the Griffin sills are poorly connected (Figs. 6–8), forming tongues that branch and coalesce close to the paleohorizontal (Fig. 9). Although some continue laterally for up to 40 km, most sills are generally difficult to trace for greater than 10 km in any two-dimensional set of exposures, typically tapering toward blunt terminations (Figs. 7 and 8). In some areas, multiple sills occur at different stratigraphic levels in the same section (e.g. Fitzpatrick Lake, Fig. 7). However, along The Grey Hills three separate sills are staggered in an en echelon array, with minimal overlap between individuals (Fig. 8). The sills at The Grey Hills also climb upsection within the Ameto Formation (from southeast to northwest, Fig. 8) although in general, such changes in stratigraphic level cannot be traced. For example, between Fitzpatrick Lake and Sealhole Lake the sills rise 2–3.5 km across a distance of 10 km, but continuous step-ups from east to west are lacking. These sills terminate within the Montgomery Group and Maguse Member on the southeast without an obvious connection to those in the Ameto Formation to the west (Fig. 7).

3.3. Dykes

Absent in central Hurwitz Basin, dykes have only been recognized at three sites (Figs. 7 and 10), close to Fitzpatrick Lake at the southern edge of the Griffin suite (Fig. 2). First, northeast of Fitzpatrick Lake, a northeast-trending 20 m-wide dyke cuts south-dipping Maguse Member beds above the highest of two Griffin sills (Fig. 10). Because of faulting and lake cover, it is unclear if this dyke leads upward, breaking away from the roof of the highest sill, or if it connects in the third dimension as a feeder to both sills. Second, on the south shore of the north arm of Fitzpatrick Lake, two 20 m-wide northeast-trending dykes cut Montgomery Group strata, but neither connects to a

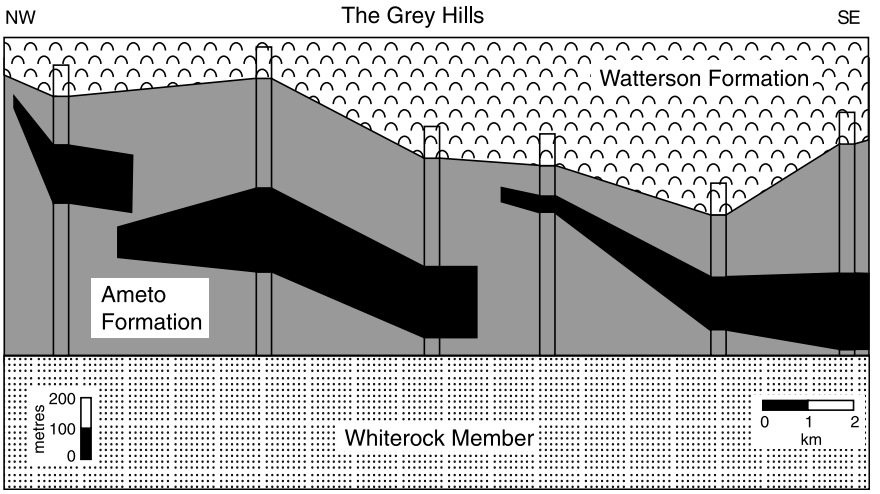

Fig. 8. Stratigraphic section along The Grey Hills illustrating three en-echelon sills, each climbing upsection in the Ameto Formation. Based on 1:50 000-scale mapping (Aspler et al. 1992, 1994). See Figs. 2 and 4 for location.

sill (Fig. 10). Third, extending north from an east-trending arm of Fitzpatrick Lake, a 40 m-wide dyke containing plagioclase megacrysts cuts perpendicular to the trace of east-trending (pre-Hurwitz Group) folds in the Montgomery Group (Fig. 10). This dyke bends eastward through 90°, becomes concordant with bedding, and widens to become a 200 m-thick megacryst-bearing inclined sheet (Fig. 10), similar to dyke-to-sill roll-overs described elsewhere (Hyndman and Alt, 1987).

The absence of feeder dykes elsewhere in Hurwitz Basin does not merely reflect poor exposure; if present, such dykes would be easily recognizable on the relatively continuous and lichen cover-free white-toned ridges formed by quartz arenites of the Whiterock Member. In short, dykes associated with the Griffin sills are rare, and physical continuity between a dyke and a sill has only been established in one example.

3.4. Contacts

Contacts between the gabbros and host units are sharp: the gabbros have well-defined chilled margins, and pelitic country rocks are hornfelsed

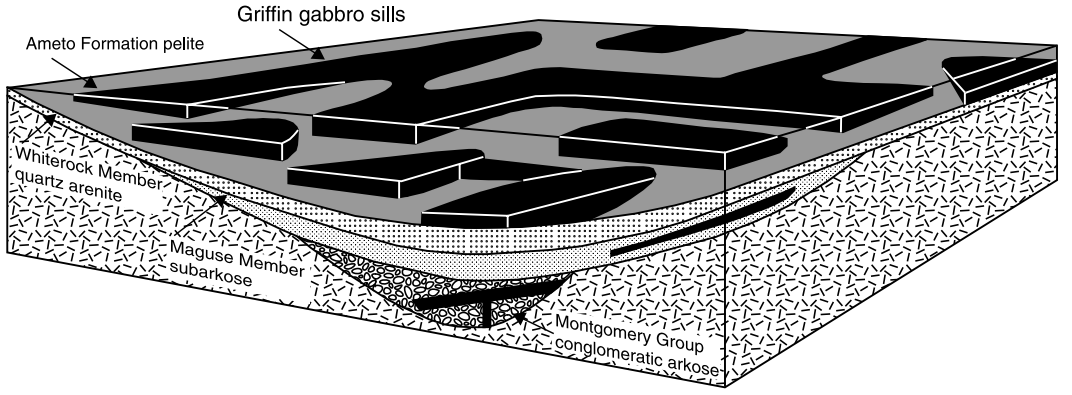

Fig. 9. Cartoon illustrating inferred sill geometry. Rather than forming sheets that are continuous in three dimensions, the sills are tongue-like tabular bodies exhibiting limited continuity in two dimensional sections perpendicular to the paleohorizontal.

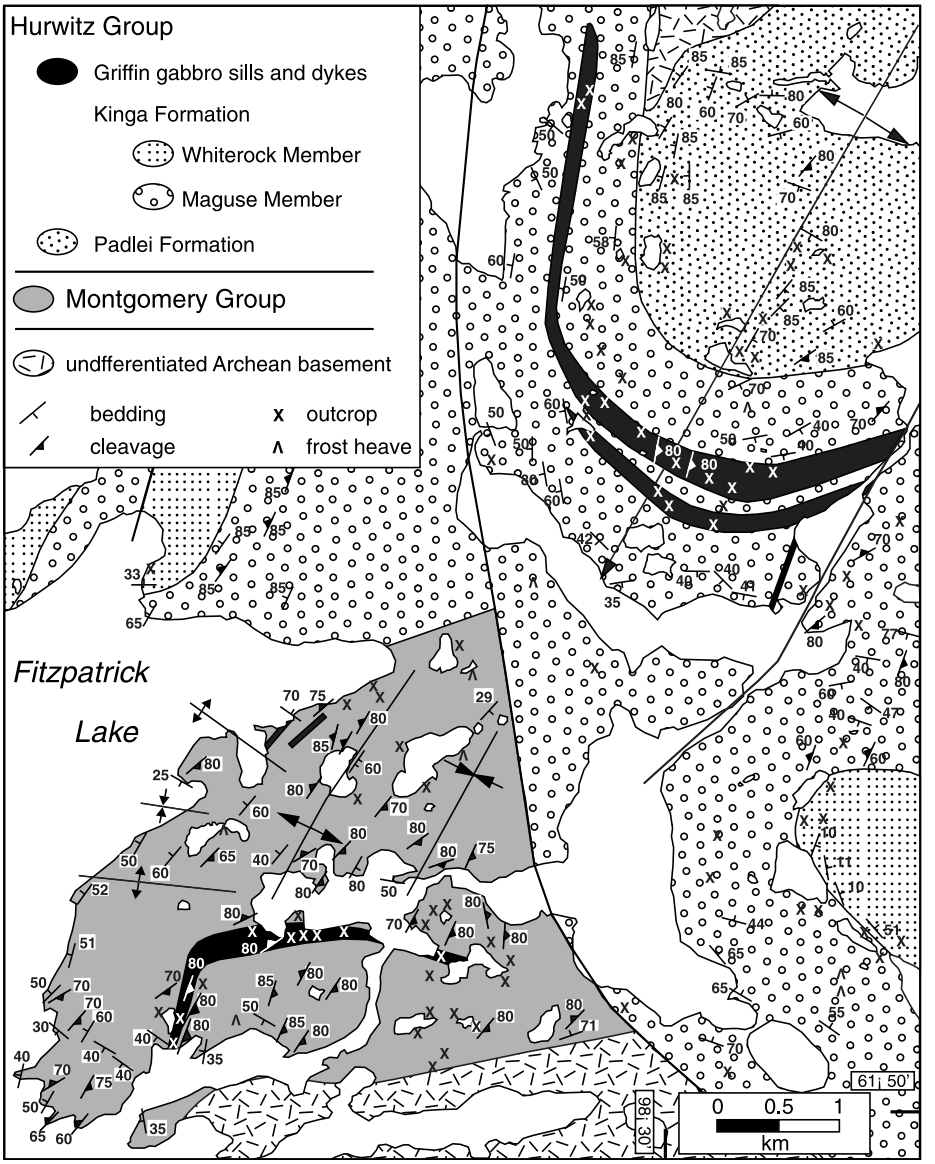

Fig. 10. Geological map, eastern Fitzpatrick Lake, illustrating potential feeder dykes and associated sills cutting the Montgomery Group and Hurwitz Group (Maguse Member). After Aspler et al. (2000). See Figs. 2 and 4 for location.

within a metre of the gabbros. Metre-scale bifurcations of gabbro locally extend from sill margins into host rocks. Thinly interbedded siltstones and mudstones of the Ameto Formation in contact with the gabbros lack soft-sediment deformation structures. The gabbros contain xenoliths of Ameto Formation pelites that are angular, have sharp boundaries, and display undistorted internal lamination, and peperites are lacking. As will be discussed further below, these observations imply that the Ameto Formation was well indurated before gabbro emplacement, and that the sills are not coeval with volcanic rocks of the Happotiyik Member (cf. Bell, 1968, 1970).

3.5. Structure and petrography

The sills are typically massive, generally consisting of uniformly medium- to coarse-grained plagioclase (variably altered to sericite and epidote) and primary hornblende (variably altered to chlorite). They generally lack a penetrative cleavage related to regional folding, but are well-jointed; many joint surfaces are covered by chlorite slickenfibres. Host rock xenoliths are uncommon, and occur in narrow zones immediately adjacent to sill margins. Exotic xenoliths derived from Archean basement have not been observed. In some areas, such as at Griffin Lake, the sills display well-defined joints subparallel to adjacent strata (Fig. 5), possibly reflecting an anisotropy inherited from subtle primary magmatic layering.

At Fitzpatrick and Sealhole lakes, the gabbros contain plagioclase megacrysts in proportions ranging from a few crystals to 20% (Fig. 11). The megacrysts are subhedral to euhedral, tabular to equant, single crystals (locally broken) with maximum dimensions of 1–10 cm. At Fitzpatrick Lake, the megacrysts are dispersed randomly in a fine- to medium-grained groundmass. Similar to examples described from the Mesoproterozoic Gardar intrusions in Greenland (Bridgwater, 1967), both the inclined sheet in the Montgomery Group and the dyke that rolls into it (Fig. 10) are megacryst-bearing, indicating that the megacrysts were transported from elsewhere and not did not result from in situ growth. In a thick (1000 m) sill at Sealhole Lake, the megacrysts are layered in zones (Fig. 11) that are sub-parallel to bedding in overlying and underlying Hurwitz Group strata. These layers are defined mainly by variation in plagioclase size and concentration, and range from zones of single aligned crystals several cm thick, to massive m-scale beds. Some of the thicker layers display normal size grading (Fig. 11B). In addition, some display mineralogical grading, with local basal zones concentrated with cm-sized hornblende crystals. By analogy to the Fitzpatrick Lake occurrences, we suggest that the megacrysts at Sealhole Lake were transported by magmatic flow and that the layering was produced by gravitational settling and/or current sedimentation, although we cannot dismiss the possibility of a contribution by in situ growth (Ashwal, 1993; Naslund and McBirney, 1996 for review). As will be returned to below, the megacryst-bearing gabbros also display the strongest geochemical and isotopic contamination signatures, and we consider that the megacrysts were entrained from the crystal mush of a regionally unique magma chamber, and transported laterally in magma flow pulses.

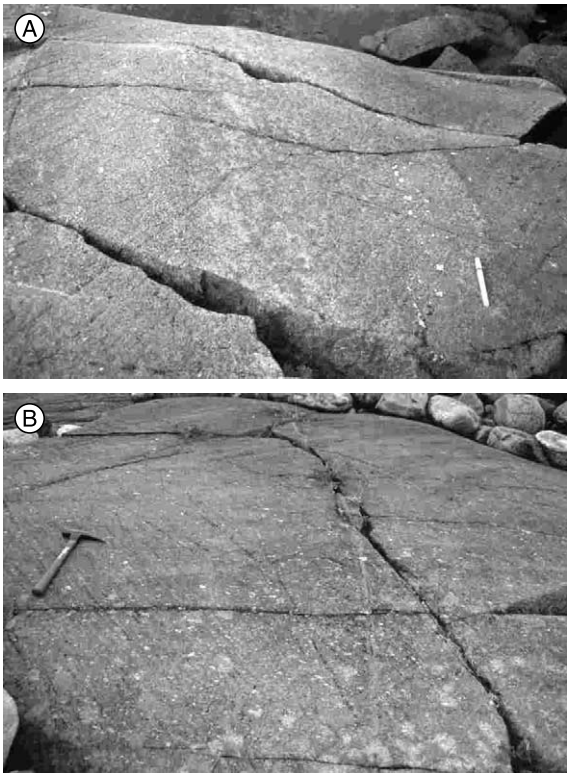

Fig. 11. Layered plagioclase megacryst-bearing sill, east shore of Sealhole Lake. (A) Dispersed plagioclase megacrysts distributed in layers. (B) Normal grading defined by decrease in size and concentration of megacrysts to top of photo.

3.6. Geochemical and Sm–Nd isotopic studies

3.6.1. Major and trace elements

Samples from the central part of Hurwitz Basin, have compositions that plot in the alkaline basalt-trachybasalt field of a total alkali-silica diagram (Fig. 12; Table 1). In contrast, several samples from the southeast have higher SiO_2, and plot in

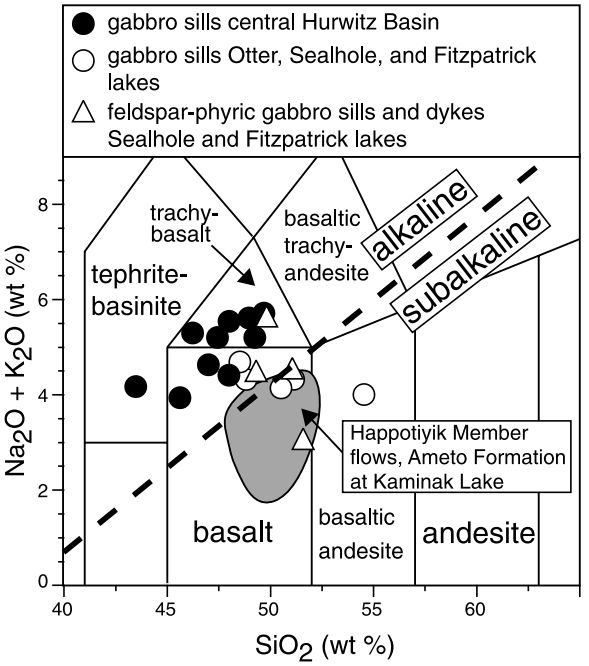

Fig. 12. Griffin gabbro sill and dyke samples plotted on a total alkali-silica classification diagram of le Bas et al. (1986). Field for basaltic-gabbroic flows in Ameto Formation at Kaminak Lake (Happotiyik Member) from Hemmingway and Sandeman (1999).

the subalkaline basalt and basaltic andesite fields (Fig. 12). Relative to primary mantle melts (Basaltic Volcanism Study Project, 1981), MgO values are low (average 5.20 wt.%; $n = 19$) implying that the magmas fractionated after melting. Concentrations of TiO_2 average 3.50 wt.% ($n = 19$), and concentrations of both the compatible (e.g. Ni, V, Sc) and incompatible (e.g. Ti, P, La) elements display wide scatter with respect to Mg number (Fig. 13).

Differences in bulk composition between sills in the central part of Hurwitz Basin and those in the southeast are reflected by markedly different incompatible element patterns (Fig. 14, normalized to Primitive Mantle). Sills from central Hurwitz Basin display patterns similar to modern hotspot-related ocean island basalts (Sun and McDonough, 1989; Weaver, 1991), with enrichments in Nb and La producing gently convex-upward curves (Fig. 14A). In contrast, sills and dykes to the southeast yield variably negative Nb anomalies (Fig. 14B) characteristic of continental volcanic sequences that have been contaminated by crustal material (Dupuy and Dostal, 1984; Arndt et al., 1993; Griselin et al., 1997). All samples have patterns with steep negative slopes owing to depletions in the heavy REE.

3.6.2. Sm–Nd isotopes

Values for ε_{Nd}^{2111} from sills in the central part of the basin are relatively uniform, and range from -0.1 to $+1.0$ (Table 2, Fig. 15). Sills and dykes in the southeast display a wider variation in ε_{Nd}^{2111} ($+0.5$ to -3.6), and an inverse correlation between ε_{Nd}^{2111} and SiO_2 (Table 2, Fig. 15). In samples from central Hurwitz Basin, ε_{Nd}^{2111} is independent of TiO_2 and P_2O_5, whereas those from the southeast display a weak positive correlation (Fig. 16).

3.6.3. Griffin gabbros compared with Happotiyik Member flows

These two units have significant geochemical differences, consistent with field observations (see above) that the Griffin gabbro sills and dykes formed after the Ameto Formation was well indurated, and could not be coeval with the Happotiyik Member mafic flows: (1) the Griffin sills are typically alkaline, whereas the Happotiyik flows are subalkaline (Fig. 12); (2) the Griffin sills and dykes have greater overall REE abundances than the Happotiyik Member (Fig. 14); (3) Griffin sills in the central part of Hurwitz Basin display enrichments in Nb and La whereas the Happotiyik flows display negative Nb anomalies (Fig. 14A); (4) the Griffin sills and dykes have greater depletions in the heavy REE than the Happotiyik flows, and hence steeper incompatible element patterns (Fig. 14); (5) the Griffin sills typically have positive Ti anomalies and high TiO_2 values (average 3.50 wt.%, $n = 19$), whereas the flows have weak negative Ti anomalies (TiO_2 average, 1.20, $n = 6$; Hemmingway and Sandeman, 1999, Fig. 14); and (6) the MgO contents of the Griffin sills and dykes (average 5.20 wt.%; $n = 19$) are lower than those of the Happotiyik flows (average 6.80 wt.%; $n = 6$; Hemmingway and Sandeman, 1999), indicating that the sills are more highly fractionated.

Table 1
Major and trace element geochemistry, Griffin gabbro sills and dykes

Sample	93-4-2e	93-5-7d	93-16-12	93-52-35	93-37-1	98-12-3	98-19-1	98-22-1	98-22-2	98-22-5	98-22-7	98-22-8	98-22-9	99-4-13b	99-8-3	99-8-11	99-14-8	99-19-13	99-28-25	Precision
Area	Otter	Otter	Otter	Mont-gomery	Ducker	Mont-gomery	Ameto	Grey Hills	Ducker	Hawk Hill	Watterson	Griffin	Griffin	Fitz-patrick	Sealhole	Sealhole	Fitz-patrick	Sealhole	Fitz-patrick	
Unit	Sill	Sill	Sill	Sill	Sill	Sill	Sill	Sill	Sill	Sill	Sill	Sill	Sill	Dyke	Phyric sill	Phyric sill	Phyric dyke	Sill	Phyric sill	
wt.%																				
SiO_2	48.54	49.76	49.89	44.18	41.52	46.88	45.64	48.45	46.61	46.75	48.67	47.56	46.81	53.69	49.12	50.48	48.32	48.2	51	0.23
TiO_2	3.83	3.84	1.29	5.6	4.34	4.14	4.82	4.03	3.35	3.51	3.84	2.86	3.64	1.873	3.49	2.53	3.8	4.1	1.29	0.03
Al_2O_3	13.3	13.66	15.46	14.29	14.53	12.43	13.51	13.96	14.24	12.72	13.35	16.18	15.38	12.74	14.67	15.8	13.12	13.31	14.68	0.12
Fe_2O_3	16.32	15.55	12.85	16.59	13.08	16.49	16.97	15.13	12.57	16.74	15.74	13.59	15.08	15.82	14.03	12.1	16.52	16.83	14.07	0.12
MnO	0.21	0.21	0.18	0.2	0.03	0.16	0.21	0.20	0.12	0.21	0.19	0.17	0.17	0.201	0.17	0.16	0.21	0.2	0.21	0.01
MgO	4.72	3.77	6.26	5.17	11.76	4.14	4.49	4.03	5.61	6.50	4.54	5.76	5.64	3.33	3.91	4.48	4.45	4.52	5.36	0.05
CaO	7.15	7.5	7.55	6.65	0.96	6.84	7.10	7.13	5.85	6.50	6.87	8.37	7.80	6.59	7.38	8.54	7.57	7.2	9.06	0.13
Na_2O	3.57	2.94	3.52	3.72	0.01	4.04	3.47	4.39	3.09	2.85	2.62	3.23	3.31	2.74	3.59	3.31	2.91	3.25	2.33	0.04
K_2O	0.8	1.23	0.86	0.09	3.99	1.38	1.79	1.21	2.30	2.30	2.50	1.14	1.32	1.17	1.93	1.14	1.42	1.28	0.65	0.03
P_2O_5	0.34	0.38	0.09	0.42	0.38	1.13	0.69	0.40	0.38	0.39	0.44	0.34	0.43	0.27	0.31	0.28	0.45	0.43	0.16	0.07
LOI	0.15	0.43	0.7	1.62	9.22	1.37	0.61	0.77	4.96	1.14	0.47	0.30	0.34	0.9	1.5	2	1.4	1.8	0.9	0.08
Total	98.93	99.27	98.65	98.53	99.77	99.00	99.30	99.70	99.08	99.61	99.23	99.50	99.92	99.32	100.1	100.82	100.17	101.12	99.71	
S	0	0.04	0.06	0.04	5.33	0.01	0.01	0.03	0.08	0.01	0.01	0.04	0.01	nd	nd	nd	nd	nd	nd	0.01
CO_2	0.18	0.56	0.13	0.04	0.32	0.28	0.22	0.23	3.62	0.1	0.13	0.06	0.08	nd	nd	nd	nd	nd	nd	0.07
ppm																				
Nb	18	20	6	15	17	31.14	22.72	23.13	23.27	22.13	24.74	20.08	25.26	11	15	15	23	22	6	1
Zr	219	243	105	144	127	240	174	205	203	207	252	178	230	194	176	163	230	209	124	3
Y	30	33	22	23	21	42	27	29	34	33	38	27	35	30	21	20	30	28	20	2
Sr	526	522	217	598	19	373.6	533.9	475.7	292.8	405.8	562.1	597.8	577.1	311	603	712	585	546	271	13
Rb	33	46	30	9	48	25.73	50.16	34.18	76.67	92.32	107.14	39.74	40.24	24	53	21	48	41	13	2
Ba	315	429	277	111	193	nd	nd	nd	nd	nd	nd	nd	nd	683	540	413	446	419	267	30
Cr	47	37	36	10	8	nd	nd	nd	nd	nd	nd	nd	nd	36	40	66	43	74	53	9
Co	50	40	50	54	75	33	40	45	47	59	50	51	45	46	35	37	46	46	58	4
Cu	30	67	20	30	29	83	92	50	71	48	53	66	15	nd	nd	nd	nd	nd	nd	7
Ni	65	40	65	72	108	22	41	55	95	105	57	117	84	63	42	55	48	49	116	4
Sc	24	24	27	20	4	26	25	26	22	22	24	19	24	nd	nd	nd	nd	nd	nd	2
V	370	360	250	300	219	210	298	429	299	345	371	270	307	218	443	312	400	449	215	7
Zn	120	120	110	130	43	127	148	161	98	154	125	124	142	125	111	92	130	131	104	8
La	28	35	14	22	21.075	42.50	27.21	25.82	26.80	28.29	32.50	24.45	30.22	30.14	23.40	21.97	31.07	27.93	19.13	0.11
Ce	66	80	31	53	52.52	98.91	64.35	61.38	60.50	64.75	74.30	55.45	68.50	59.32	53.17	48.42	70.21	63.92	37.88	0.2
Pr	9.1	11	4.1	7.5	7.08	14.63	9.45	8.69	8.53	9.06	10.52	7.73	9.66	7.52	7.33	6.59	9.91	9.11	4.84	0.08
Nd	40	47	17	33	31.67	65.67	41.64	37.41	36.64	38.86	44.66	32.95	41.34	29.65	30.02	27.99	42.93	39.44	19.54	0.31
Sm	8.9	10	4.2	7.2	6.51	13.92	9.05	8.36	7.73	8.42	9.71	6.95	8.80	6.17	6.59	5.93	9.32	8.62	4.31	0.09
Eu	2.9	3.2	1.4	2.6	2.02	4.68	3.40	2.81	2.46	2.59	2.96	2.33	2.54	1.56	2.15	2.08	2.94	2.89	1.34	0.04
Gd	8.1	9.4	4.3	6.4	4.85	11.74	7.71	7.27	6.63	7.38	8.38	6.04	7.62	5.75	5.74	5.25	8.21	7.53	4.12	0.1
Tb	1.2	1.4	0.65	0.86	0.6	1.56	1.04	1.06	0.96	1.02	1.20	0.86	1.09	0.89	0.84	0.75	1.16	1.05	0.64	0.08
Dy	6	6.9	3.8	4.4	3.27	8.51	5.70	5.97	5.53	5.91	6.75	4.96	6.40	5.55	4.74	4.28	6.43	5.79	4.06	0.04
Ho	1.1	1.2	0.75	0.75	0.56	1.49	1.00	1.10	1.02	1.05	1.23	0.93	1.17	1.16	0.90	0.78	1.22	1.12	0.91	0.06
Er	2.9	3.2	2.1	1.9	1.46	3.84	2.52	2.77	2.74	2.69	3.18	2.48	3.13	3.33	2.26	2.07	3.08	2.78	2.50	0.02
Tm	0.35	0.38	0.28	0.22	0.18	0.47	0.30	0.34	0.36	0.34	0.39	0.32	0.40	0.48	0.29	nd	0.40	0.36	0.35	0.01
Yb	2.2	2.5	1.9	1.5	1.1	2.70	1.77	2.00	2.19	1.94	2.29	1.94	2.32	3.00	1.69	1.55	2.31	2.07	2.25	0.05
Lu	0.29	0.34	0.27	0.2	0.17	0.41	0.24	0.27	0.32	0.27	0.34	0.27	0.35	0.48	0.26	0.24	0.36	0.31	0.36	0.02
Th	3.8	4.5	2	2.1	1.56	3.18	2.13	3.08	2.53	3.05	3.64	2.23	2.88	7.57	3.42	3.04	3.75	3.32	4.38	0.1

Table 1 (*Continued*)

Sample	93-4-2e	93-5-7d	93-16-12	93-52-35	93-37-1	98-12-3	98-19-1	98-22-1	98-22-2	98-22-5	98-22-7	98-22-8	98-22-9	99-4-13b	99-8-3	99-8-11	99-14-8	99-19-13	99-28-25	Precision
Area	Otter	Otter	Otter	Mont-gomery	Ducker	Mont-gomery	Ameto	Grey Hills	Ducker	Hawk Hill	Watterson	Griffin	Griffin	Fitz-patrick	Sealhole	Sealhole	Fitz-patrick	Sealhole	Fitz-patrick	
Unit	Sill	Sill	Sill	Sill	Sill	Sill	Sill	Sill	Sill	Sill	Sill	Sill	Sill	Dyke	Phyric sill	Phyric sill	Phyric dyke	Sill	Phyric sill	
U	0.88	1	0.34	0.51	3.66	0.74	0.48	0.72	0.56	0.73	0.86	0.52	0.65	1.61	0.84	0.77	0.92	0.83	1.02	0.12
Hf	3.8	4.7	1.8	3.4	3.29	5.81	2.53	3.41	4.51	4.36	5.43	2.84	4.20	5.01	4.53	3.92	5.90	5.42	3.31	0.1
Ta	1.4	1.5	0.41	1.2	0.34	1.92	1.47	1.48	1.46	1.43	1.59	1.27	1.64	0.63	1.02	0.90	1.50	1.35	N.D.	0.02

Analyses of phyric samples include both groundmass and plagioclase megacrysts. Precisions are based on analyses of standards and blind duplicates. See Appendix A for methods.

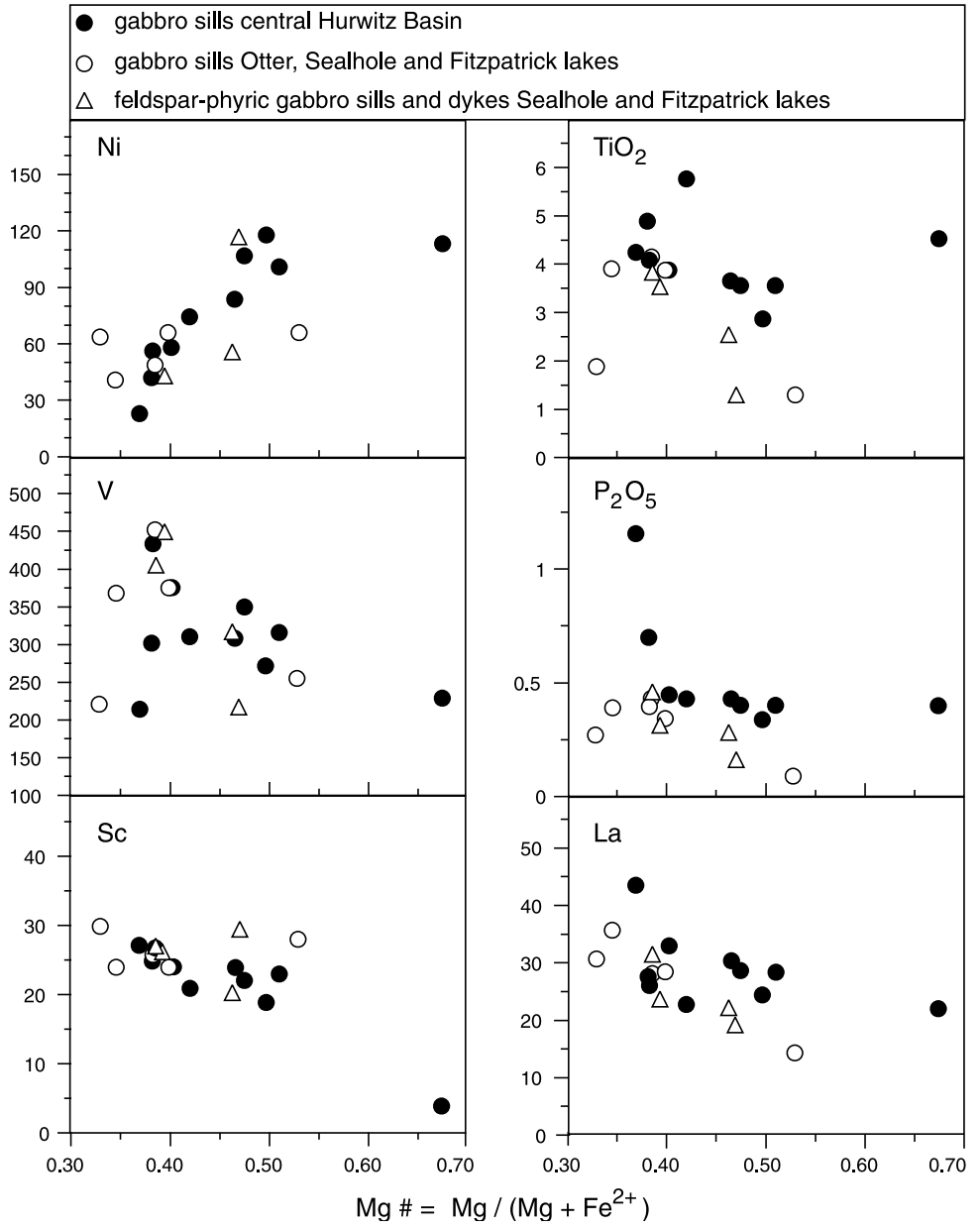

Fig. 13. Plots of compatible (Ni, V, Sc) and incompatible (Ti, P, La) element concentrations with respect to Mg number (calculated with cation proportions; volatile-free). Although Ni and La are weakly correlated to Mg#, all elements display a wide scatter, inconsistent with derivation in a direct line of descent from a common parent due to fractional crystallization.

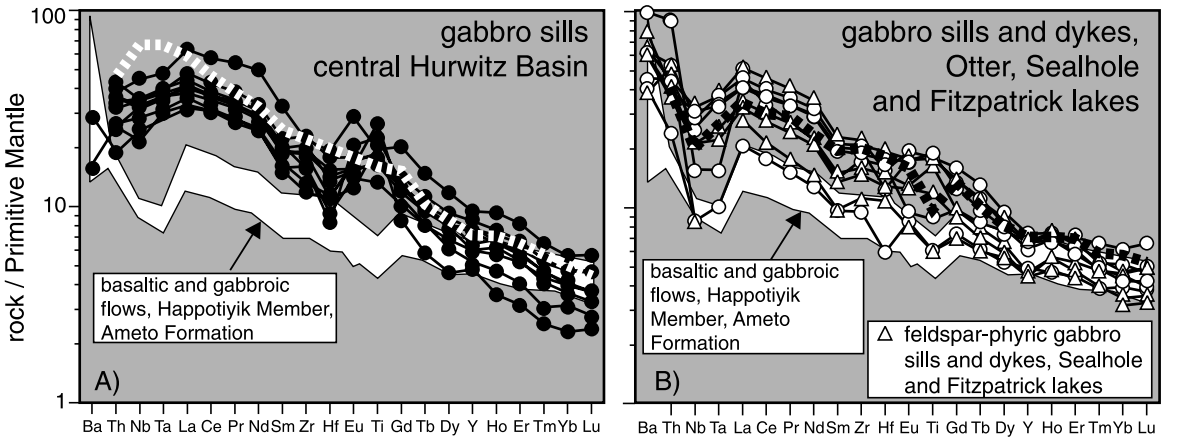

Fig. 14. Incompatible elements in Griffin gabbro sills and dykes normalized to Primitive Mantle (Sun and McDonough, 1989). (A) Samples from central Hurwitz Basin. Envelope for basaltic flows in the Ameto Formation at Kaminak Lake (Happotiyik Member) from Hemmingway and Sandeman (1999). Thick dashed white line represents ocean island basalts for comparison (from Sun and McDonough, 1989). (B) Samples from southeastern exposures, near Otter, Sealhole and Fitzpatrick lakes. Thick dashed black line represents crustally contaminated flows near the base of the Coppermine River basalts, 1.27 Ga Mackenzie igneous event for comparison (after Griselin et al., 1997).

Table 2
Sm–Nd isotope data, Griffin gabbro sills and dykes

Sample	Area/unit	Nd (ppm)	Sm (ppm)	$^{147}Sm/^{144}Nd$	$^{143}Nd/^{144}Ndm$	$^{143}Nd/^{144}Ndi$	ε_{Nd}^{T}*	$T^{*}_{(DM)}$*
93-4-2e	Otter sill	35.60	7.93	0.1347	0.511789	0.509916	0.3	2535
93-5-7d	Otter sill	45.89	10.05	0.1324	0.511766	0.509925	0.4	2507
93-16-12	Otter sill	18.73	4.35	0.1405	0.511767	0.509813	−1.8	2780
93-52-35	Montgomery sill	39.42	8.48	0.1301	0.511748	0.509940	0.7	2470
93-37-1	Ducker sill	30.22	6.36	0.1272	0.511695	0.509927	0.5	2480
98-12-3	Montgomery sill	61.34	13.26	0.1307	0.511764	0.509947	0.9	2459
98-19-1	Ameto sill	42.88	9.44	0.1332	0.511791	0.509940	0.7	2484
98-22-1	Grey Hills sill	35.97	8.11	0.1362	0.511795	0.509901	−0.1	2574
98-22-2	Ducker sill	34.43	7.49	0.1316	0.511772	0.509943	0.8	2471
98-22-5	Hawk Hill sill	39.93	8.85	0.1340	0.511784	0.509922	0.4	2522
98-22-7	Watterson sill	43.63	9.59	0.1328	0.511779	0.509933	0.6	2495
98-22-8	Griffin sill	32.12	6.93	0.1304	0.511769	0.509955	1.0	2444
98-22-9	Griffin sill	38.77	8.39	0.1308	0.511770	0.509952	1.0	2451
99-4-13b	Fitzpatrick dyke	29.41	6.22	0.1278	0.511499	0.509722	−3.6	2840
99-8-3	Sealhole phyric sill	29.30	6.43	0.1327	0.511724	0.509879	−0.5	2595
99-8-11	Sealhole phyric sill	26.83	5.81	0.1310	0.511706	0.509886	−0.4	2572
99-14-8	Fitzpatrick phyric dyke	41.26	9.11	0.1335	0.511784	0.509928	0.5	2508
99-19-13	Sealhole sill	37.25	8.22	0.1334	0.511778	0.509924	0.4	2514
99-28-25	Fitzpatrick phyric sill	18.51	4.06	0.1326	0.511606	0.509762	−2.8	2810

Analyses of phyric samples include both groundmass and plagioclase megacrysts. See Appendix A for methods. Note: $^{143}Nd/^{144}Ndm$ = measured present-day ratio, $^{143}Nd/^{144}Ndi$ = intial ratio assuming crystallization age (T) of 2111 Ma. *Epsilon Nd value: $\varepsilon_{Nd}^{T} = (((^{143}Nd/^{144}Ndi)/(^{143}Nd/^{144}NdCHUR)) - 1)*10{,}000$; CHUR = chondritic meteorites at time T. $T_{(DM)}$** is depleted mantle model age, assuming depleted mantle $^{147}Sm/^{144}Nd = 0.214$ and present-day $^{143}Nd/^{144}Nd = 0.513115$.

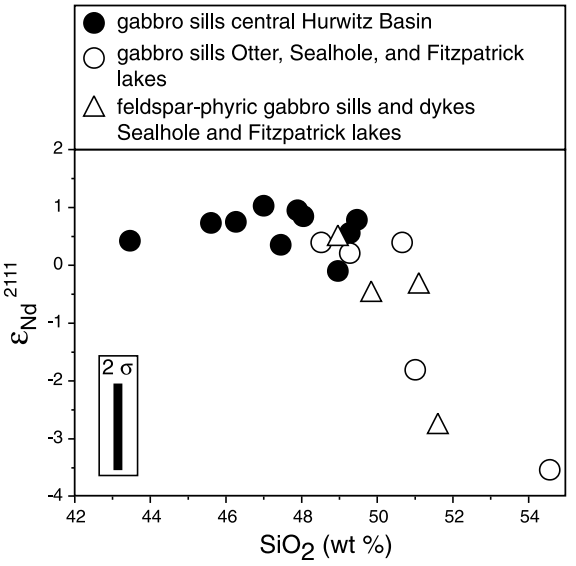

Fig. 15. Summary of ε_{Nd}^{2111} versus SiO_2 for Griffin gabbro samples. In central Hurwitz Basin, ε_{Nd}^{2111} and SiO_2 are independent, whereas samples from Otter, Sealhole, and Fitzpatrick lakes display a negative correlation, indicating crustal contamination.

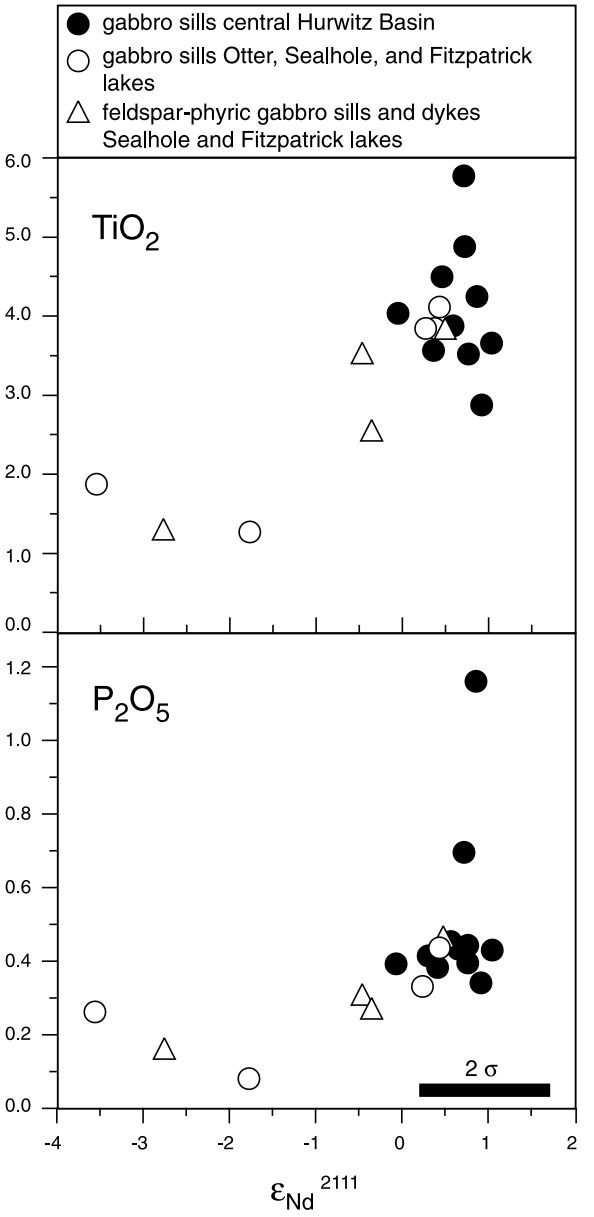

Fig. 16. TiO_2 and P_2O_5 versus SiO_2 for Griffin gabbro sill and dyke samples. In central Hurwitz Basin, TiO_2 and P_2O_5 are not correlated with SiO_2, whereas samples from Otter, Sealhole, and Fitzpatrick lakes display a positive correlation, indicating crustal contamination. Analytical uncertainties are less than symbol size.

4. Discussion

4.1. Magma sources

Like many continental mafic suites, such as the ~1.27 Ga Mackenzie dykes and Coppermine basalts in northern Canada (Baragar et al., 1996; Griselin et al., 1997), the 250 Ma Siberian Traps (Fedorenko et al., 1996), and the 65 Ma Deccan Traps in western India (Hawkesworth and Gallagher, 1993), gabbro sills in the central part of Hurwitz Basin display geochemical and isotopic characteristics that are typical of modern hotspot-related ocean island basalts (see above). With incompatible element enrichments and low ε_{Nd}^{2111} values, the gabbros appear to have been derived from enriched asthenosphere sources. The lack of systematic variation in ε_{Nd}^{2111} with SiO_2 implies that crustal contamination was not a major process affecting the magmas in central Hurwitz Basin, consistent with the near absence of xenoliths. Heavy REE depletions, together with high TiO_2 concentrations, point to derivation of small magma volumes by low-degree partial melting of garnet-bearing peridotite sources at depths of ~70–100 km (Ellam, 1992; Arndt et al., 1993;

Nykänen et al., 1994). The sills cannot be related in a single line of descent from a single parental magma due to fractional crystallization because both compatible and incompatible elements display wide scatter with respect to Mg number. This is consistent with derivation from different magma chambers originating from the same mantle plume, such has been suggested for the Mackenzie dykes by Baragar et al. (1996).

Although crustal components do not appear to have contributed significantly to the sills in the central part of Hurwitz Basin, sills and dykes near the southern limit of the Griffin gabbros, particularly those containing plagioclase megacrysts, were contaminated by crustal material, as indicated by negative ε_{Nd}^{2111} values, an inverse correlation between ε_{Nd}^{2111} and SiO_2, and positive correlations between ε_{Nd}^{2111} and TiO_2 and P_2O_5. The decrease in contamination from southeast to northwest may reflect a temporal or 'downstream' increase in the degree to which magmas were mechanically insulated from country rock, such as suggested to explain contamination patterns elsewhere (Wirth and Vervoort, 1995; Baragar et al., 1996). However, close coincidence of contamination with distribution of plagioclase megacrysts suggests a common process. We interpret that the sills and dykes in the south were drawn from a regionally unique, contaminated magma chamber in which temporarily stored magmas crystallized plagioclase crystals that were periodically entrained and transported during forceful magma flow events, similar to mechanisms envisaged by Phinney et al. (1988), Hansen and Grönvold (2000), Phinney and Halls (2001).

4.2. Subjacent or external magma derivation?

A wide spectrum of relationships exists between potential feeder dykes and sills (Ernst and Buchan, 1997b). In many cases, dykes are restricted to the margins of sedimentary basins (Francis, 1982), but this is not universal (Leaman, 1995). In some examples, such as the Karoo sills (Jurassic) in southern Africa (Chevallier and Woodford, 1999), or the Roraima intrusive suite (Paleoproterozoic) in the Guiana shield (Gibbs, 1987), sills and dykes are intimately connected in complex three-dimensional networks. In others, such as the Mackenzie sills ($\sim$1.27 Ga) in northern Canada (Hulbert et al., 1993; Mandler and Clowes, 1997), or the Paranà sills (Cretaceous) in South America (White, 1992; Peate, 1997), large sills are connected to dykes that form parts of giant radiating swarms. In still others, such as the Nipissing sills ($\sim$2.2 Ga) in Ontario, no physical connection can be made between sills in Huronian Supergroup strata (Paleoproterozoic) and coeval dykes in Archean basement that form a giant radiating swarm (Klotz, Maguire, and Senneterre dykes; Buchan et al., 1998). Finally, the Ferrar sills (Jurassic) of Antarctica, although linked by numerous small dykes, continue laterally for $\sim$3000 km and connections to feeder dykes in basement have not been observed (Hamilton, 1965; Fleming et al., 1997; Elliot et al., 1999). Similar to the Ferrar example, feeder dykes are unknown in Archean basement to the Hurwitz Group. What few dykes have been found are not part of a regional swarm, are restricted to the southern limit of the Griffin suite, and can be shown to connect with a sill in only one example. Hence, the geometry of the sills and sill–dyke relationships established by field mapping indicate that the magmas moved laterally from a source outside of Hurwitz Basin.

As outlined below, geochemical and isotopic data from $\sim$1.83 to 1.81 Ga ultrapotassic dykes and flows of the Christopher Island Formation that formed early in the history of Baker Lake Basin (Fig. 2) also imply the mantle reservoir that produced the Griffin gabbros was well removed from Hurwitz Basin, and from the central Hearne domain. Ultrapotassic rocks such as the Christopher Island Formation minettes, characterized by high volatile contents, subduction zone-like incompatible element enrichment patterns, and distinctive isotopic compositions, are widely accepted as melts of metasomatized lithospheric mantle (Canning et al., 1998). Incompatible element patterns and ε_{Nd}^{1830} values of the Christopher Island Formation minettes are remarkably uniform across a large area (240 000 km^2) of the western Churchill Province (Cousens et al., 2001). This geochemical and isotopic homogeneity indicates that a correspondingly large and uniform reservoir

of enriched lithospheric mantle extended beneath the western Churchill, including parts of central Hearne domain crust that contain the Griffin gabbros (Cousens et al., 2001). With Nd model ages of ~2.8 Ga, and highly negative ε_{Nd}^{1830} values (80% between −7 and −9) that reflect neither crustal contamination nor Paleoproterozoic subduction, this reservoir was probably created during a Neoarchean metasomatic event, and was tapped during lithospheric stretching at ~1.83 Ga (Cousens et al., 2001). If such a volatile-rich sheet was frozen within, or close to the base of, the lithospheric mantle beneath the central Hearne domain at the end of the Archean, then post-Archean magmatic suites derived from sub-central Hearne mantle should display the geochemical and isotopic enrichment signatures that characterize the Christopher Island Formation (Cousens et al., 2001). Two such suites, the ~2.45 Ga Kaminak dykes and Spi Group flows and the Tulemalu-MacQuoid dykes (~2.19 Ga; Fahrig et al., 1984; Tella et al., 1997) display negative ε_{Nd}^{T} values and subduction zone-like enriched incompatible element patterns that include prominent negative Nb, Ta, P, and Ti anomalies, consistent with derivation, at least in part, from the same enriched source as the Christopher Island Formation (Sandeman et al., 2000; Cousens et al., 2001). The Griffin gabbros fail to show evidence of this Neoarchean subduction-like enrichment event. They display hotspot-like ε_{Nd}^{T} values and enrichment patterns that lack negative Nb anomalies. Thus, consistent with field relationships, the geochemical data indicate that the Griffin gabbros were derived from an enriched mantle source that was outside of Hurwitz Basin and the central Hearne domain.

4.3. Manikewan ocean mantle plume?

Whereas Cenozoic dyke and sill swarms may be tracked to modern hot spots (White and McKenzie, 1989; Storey, 1995), establishing the source of Precambrian examples is more of a challenge. Nonetheless, numerous Precambrian plume centres have been identified (Ernst and Buchan, 2001a,b), and inventories of plume size, distribution, degree of clustering, and duration through geological time are being used to evaluate potential secular changes in mantle dynamics (Ernst and Buchan, in press). Because the Griffin sills cannot be related to a radiating dyke swarm, we can only speculate as to where their mantle plume source may have been, but regional relationships suggest that the most likely site was outboard of the southern Hearne margin, in what was the Manikewan ocean. Conceivably as wide as 5000 km (Symons et al., 1995), the Manikewan ocean separated the Hearne, Sask, and Superior cratons before closing during Trans-Hudson orogenesis (Fig. 1). Ongoing work indicates that rift to passive margin sedimentation along the southern flank of the Hearne domain (Yeo et al., 2000) started by at least 2075±2 Ma, the age of bimodal volcanic rocks in the lower part of the Wollaston Group (Ansdell et al., 2000). Gabbro dykes on the opposite side of Trans-Hudson orogen, near the northwestern flank of the Superior Province, have yielded similar ages (2072±3 Ma Birthday Rapids dykes; Heaman and Corkery, 1996; 2091±2 Ma Cauchon dykes Halls and Heaman, 2000). We suggest that the Griffin gabbros, volcanic rocks in the lower Wollaston Group, and the northwestern Superior dykes constitute the relics of a ~2.1 Ga mantle plume related to opening of the Manikewan ocean and circum-Superior rifting (Baragar and Scoates, 1987; St-Onge et al., 2000). Direct evidence of this plume would likely have been obscured during subsequent Trans-Hudson collisions.

4.4. Lateral magma transport from Manikewan plume

Following models proposed by McKenzie et al. (1992), White (1992), Baragar et al. (1996), we interpret that dynamic uplift above a mantle plume in what became the Manikewan ocean provided the hydraulic head for magmas to move laterally 'downhill' within the crust. According to this hypothesis, close to the plume, relatively low density melts under high magma pressures would have risen from depths of ~100 km, accumulated in discrete chambers near levels of neutral buoyancy in the middle and upper crust, and after varying degrees of fractionation, injected laterally

as dykes and sills because of the elevated topography of the focal region (Fahrig, 1987; McKenzie et al., 1992; White, 1992; Ernst and Buchan, 1997a,b, 2001a; Baragar et al., 1996; Ernst et al., 2001).

One potential problem in applying this model to the Griffin sills is that a feeder dyke swarm has not been found in the region between the Hearne margin and Hurwitz Basin. However, this is similar to the situation in the Ferrar province of Antarctica (Jurassic), where sills extend for 3000 km away from a focal region without feeder dykes in basement. For the Ferrar example, Storey and Kyle (1997) have suggested that magmas ponded in large chambers flowed away from topographic domes along the length of the Transarctic Mountains as sills. Alternatively, Fleming et al., (1997), Elliot et al. (1999) proposed that the Ferrar magmas traveled long distances in dykes that remain unexposed, owing to ice cover and level of erosion, and that these magmas were further distributed for hundreds of km as sills within flat-lying Devonian to Triassic sedimentary rocks (Beacon Supergroup) and horizontally jointed (Hamilton, 1965) granitic basement. It is possible that cryptic dykes may have extended across the southern Hearne, but have not been observed because of: (1) the deep exposure levels south of Hurwitz Basin, in southern Nunavut (Eade, 1973; Fraser, 1983) and northern Manitoba (Schledewitz, 1986), where rocks at upper amphibolite to granulite grade may have been beneath the level of dyking; (2) dyke destruction during emplacement of the Wathaman batholith (Fig. 1); (3) possible confusion of Griffin dykes with Archean dykes; and (4) extensive Quaternary drift cover. In addition, the cryptic dykes need not have formed in the high concentrations typified by, for example, the Mackenzie swarm. For example, the Abitibi swarm (1140 Ma) in central North America consists of only a few individual dykes (Ernst and Buchan, 1993), and the Senneterre dykes, which appear to have fed the Nipissing sills of northern Ontario at 2.22 Ga, are sparsely concentrated over large areas (Buchan et al., 1998).

4.5. Emplacement of sills within the Hurwitz Group

Because sills and dykes form perpendicular to σ_3 (least principal compressive stress), in the σ_1–σ_2 plane ($\sigma_1 > \sigma_2 > \sigma_3$), dykes are particularly common in areas undergoing regional horizontal extension, whereas sills tend to form in areas of regional horizontal compression (for review see Rubin, 1995; Vigneresse et al., 1999). Nonetheless, sills are common in modern rift zones (Walker, 1999), and in extensional terranes (Goodwin et al., 1989; Parsons and Thompson, 1991) where dyking alters the local stress field causing a switch in the orientations of σ_1 and σ_3, such that σ_3 becomes vertical. In addition, the differential stress required for failure is significantly reduced across anisotropies such as bedding surfaces, and under high magma pressures, sills may form perpendicular to regional σ_1 (Parsons et al., 1992; Lucas and St-Onge, 1995; Vigneresse et al., 1999; Lafrance and John, 2001). We interpret that the near-horizontal mechanical anisotropy of layered sedimentary rocks in Hurwitz Basin controlled emplacement of the Griffin sills, and that the low tensile strength of Ameto Formation mudrocks (relative to other units in the lower Hurwitz Group) coupled with high magma pressures, led to sill injection during regional extension. Upon entering the basin, magmas spread laterally as sills for several hundreds of km.

4.6. Relationship between Griffin gabbros and Happotiyik Member flows

Bell (1968, 1970) considered that the Griffin gabbro sills and the Happotiyik Member volcanic rocks (extruded during sedimentation of the Ameto Formation) formed at roughly the same time. However, both field and geochemical data presented above indicate that the Griffin gabbro sills and Happotiyik flows represent two distinct magmatic events. First, if unconsolidated at the time of gabbro injection, the Ameto sediments would have been highly susceptible to load or shock-induced thixotropy. In contrast to examples described in the literature of ubiquitous soft-sediment deformation where magmas injected into poorly consolidated sediment (McPhie, 1993;

Shaw et al., 1999), delicate layering in the Ameto Formation is preserved intact (see above). Hence we consider that emplacement of the Griffin gabbro was after lithification of the Ameto Formation. Second, the Griffin gabbros and Happotiyik Member have significant geochemical differences. In particular, the steeper incompatible element patterns of the Griffin sills (Fig. 14) imply derivation from greater depths (garnet field) than the flows (spinel field; see Ellam, 1992), the positive Ti anomalies displayed by the sills (in contrast to the weak negative Ti anomalies displayed by the flows) are consistent with melting of a deep garnet-bearing source at high pressures (Arndt et al., 1993), and the higher MgO contents of the sills indicate that they are more highly fractionated. In short, the Happotiyik flows were extruded during deposition of the Ameto Formation (sequence 2), likely at about 2.2 Ga (Aspler et al., 2001) whereas the Griffin gabbro sills were emplaced after lithification of both sequences 1 and 2, at $\sim$2.1 Ga.

5. Conclusions

- The Griffin gabbros ($\sim$2.11 Ga) are distributed discontinuously across 50 000 km^2 in the central Hearne domain of northern Canada, forming poorly connected tongue-like sills, and rare dykes, mainly within Paleoproterozoic siliciclastic strata in the lower Hurwitz Group.
- Field and geochemical data indicate that the sills were drawn from magmas from outside of Hurwitz Basin and the central Hearne domain.
- The gabbros display geochemical and isotopic characteristics of an enriched asthenosphere source, similar to many modern ocean island basalts, suggesting a mantle plume origin.
- This plume was likely situated south and east of Hurwitz Basin, beyond the present southern margin of the Hearne domain, and was active during $\sim$2.1 Ga rifting that led to opening of the Manikewan ocean, which separated the Hearne, Sask, and Superior cratons.
- Dynamic uplift above this plume provided the hydraulic head for magmas to move laterally within the crust. Lateral transport for at least 250 km across the southern Hearne domain may have occurred via cryptic dykes. Controlled by the horizontal anisotropy of sedimentary layering, magmas under high pressure spread laterally as sills upon entering Hurwitz Basin, traveling for several hundreds of km, primarily within thinly stratified mudrocks of the Ameto Formation.
- The Griffin gabbros represent a Paleoproterozic example of long-distance lateral transport of mafic magmas within the crust, analogous to the Ferrar sills (Jurassic) in Antarctica.
- Field observations and geochemical contrasts indicate that the Griffin gabbro sills and volcanic rocks in the Ameto Formation at Kaminak Lake (Happotiyik Member) represent two distinct magmatic events.

Acknowledgements

Field work was funded by the Geology Office, Indian and Northern Affairs Canada (INAC, Yellowknife) and the Geological Survey of Canada. Analytical work at Carleton University was funded by contracts from INAC and Natural Science and Engineering Research Council Canada. Preparation of the manuscript was supported by the Canada-Nunavut Geoscience Office. Samantha Siegel and Brenda Obina provided analytical assistance. We thank Ken Buchan and Richard Ernst for numerous discussions, and Richard Ernst for insightful remarks to early drafts. Comments by Journal reviewers, P.C. Lightfoot and P.C. Thurston, led to substantial improvements. This is a contribution to the Western Churchill NATMAP Project and the Canada-Nunavut Geoscience Office.

Appendix A: Analytical methods

All samples were cut into thin slabs, from which weathered rims were trimmed and discarded. The remaining material was wrapped in plastic and broken into 1-cm chips with a rock hammer. The chips were further reduced to granule size in a Bico jaw crusher, then ground to a fine powder in an agate ring mill. An aliquot of each ground sample was retained for analysis of Nd and Sm concentration and $^{143}Nd/^{144}Nd$ isotopic

composition. The remainder of the powder was sent to the Ontario Geological Survey (OGS) Geochemical Laboratories for major and trace element analysis; some samples were analyzed at the University of Ottawa X-Ray Spectrometry Facility. S and CO_2 were determined by infrared combustion (LECO furnace) at the OGS. Major element oxides were analyzed by fused-disc X-ray fluorescence (XRF) spectrometry at both labs. For samples sent to the University of Ottawa, Nb, Zr, Y, Sr, Rb, Ba, Cr, Co, Cu, Ni, V, and Zn were also determined by fused-disc XRF spectrometry. Samples sent to the OGS were analyzed for Co, Cr, Ba, Cu, Ni, Sc, V, Y and Zn by inductively-coupled plasma (ICP) emission spectrometry. All REE, Ta, Th, U, Hf, Rb, Sr, Zr and Nb determinations were by acid-dissolution ICP-mass spectrometry at the OGS. The precision of analyses is based on analyses of blind duplicates and reproducibility of in-house and international standards AGV-2, BHVO-2, BIR-1, and NBS-688.

All Sm–Nd isotopic analyses were performed at Carleton University, Ottawa (for procedures, see Cousens, 1996). Whole-rock powders were spiked with a ^{148}Nd–^{149}Sm mixture prior to dissolution. The uncertainties in Sm and Nd concentrations are ± 1–2%, but $^{147}Sm/^{144}Nd$ ratios are reproducible to better than 1%. Eighty-one runs of the La Jolla standard averaged $^{143}Nd/^{144}Nd = 0.511876 \pm 18$ (1σ, September 1992–March 2001). Epsilon Nd (ε_{Nd}^{T}) values (DePaolo and Wasserburg, 1976) were calculated relative to a modern CHUR (Chondrite Uniform Reservoir) value of 0.512638 and $^{147}Sm/^{144}Nd = 0.1967$, using measured and estimated ages. The precision of the ε_{Nd}^{T} values are ± 0.8 epsilon units, based on duplicate analyses of geochemical standards and other rock samples. Duplicate runs from this study agree within 0.5 epsilon units. Depleted mantle model (T_{DM}) ages were calculated assuming a $^{147}Sm/^{144}Nd$ of 0.2140 and $^{143}Nd/^{144}Nd$ of 0.513151 for modern depleted mantle.

References

Anderson, D.L., 1998. The scales of mantle convection. Tectonophysics 284, 1–17.

Ansdell, K.M., MacNeil, A., Delaney, G.D., Hamilton, M.A., 2000. Rifting and development of the Hearne craton passive margin: Age constraint from the Cook Lake area, Wollaston Domain, Trans-Hudson Orogen, Saskatchewan, GeoCanada 2000 Conference CD, Calgary.

Arndt, N.T., Czamanske, G.K., Wooden, J.L., Fedorenko, V.A., 1993. Mantle and crustal contributions to continental flood volcanism. Tectonophysics 223, 39–52.

Ashwal, L.D., 1993. Anorthosites. Springer-Verlag, Berlin, p. 422.

Aspler, L.B., Bursey, T.L. 1990. Stratigraphy, sedimentation, dome and basin basement-cover infolding and implications for gold in the Hurwitz Group, Hawk Hill-Griffin-Mountain Lakes area, District of Keewatin, Geol. Surv. Can. Pap. 90-1C, pp. 219–230.

Aspler, L.B., Chiarenzelli, J.R., 1996. Stratigraphy, sedimentology and physical volcanology of the Henik Group, central Ennadai-Rankin greenstone belt, Northwest Territories, Canada: Late Archean paleogeography of the Hearne Province and tectonic implications. Precambrian Res. 77, 59–89.

Aspler, L.B., Chiarenzelli, J.R., 1996. Relationships between the Montgomery Lake and Hurwitz groups, southern District of Keewatin NWT and stratigraphic revision of the lower Hurwitz Group. Can. J. Earth Sci. 33, 1243–1255.

Aspler, L.B., Chiarenzelli, J.R., 1997. Archean and Proterozoic Geology of the North Henik Lake area, District of Keewatin, Northwest Territories, Geol. Surv. Can. 1997-C, pp. 145–156.

Aspler, L.B., Chiarenzelli, J.R., 1998. Two Neoarchean supercontinents? evidence from the Paleoproterozoic. Sediment. Geol. 120, 75–104.

Aspler, L.B., Chiarenzelli, J.R., 2002. Mixed siliciclastic-carbonate ramp sedimentation in a rejuvenated Paleoproterozoic intracratonic basin: upper Hurwitz Group, Nunavut, Canada. In: Altermann, W., Corcoran, P. (Eds.), Precambrian Sedimentary Environments: a Modern Approach to Ancient Depositional Systems, International Assoc. Sedimentol. Spec. Pub. 33, pp. 293–321.

Aspler, L.B., Chiarenzelli, J.R., Cousens, B.L., McNicoll, V.J., Davis, W.J., 2001. Paleoproterozoic intracratonic basin processes, from breakup of Kenorland to assembly of Laurentia: Hurwitz Basin, Nunavut, Canada. Sediment. Geol. 141–142, 287–318.

Aspler, L.B., Chiarenzelli, J.R., McNicoll, V.J., 2002. Paleoproterozoic basement-cover infolding and thick-skinned thrusting in Hearne domain, Nunavut, Canada: intracratonic response to Trans-Hudson orogen. Precambrian Res. 116, 331–354.

Aspler, L.B., Höfer, C., Harvey, B.J.A., 2000. Geology of the Henik, Montgomery and Hurwitz groups, Sealhole and Fitzpatrick lakes area, Nunavut. Current Research, Geol. Surv. Can. 2000-C12 (CD-ROM) 10 pp.

Aspler, L.B., Chiarenzelli, J.R., Ozarko, D.L., Powis, K.B. 1994. Geology of Archean and Proterozoic supracrustal rocks in the Otter and Ducker lakes area, southern District of Keewatin, Northwest Territories, Geol. Surv. Can. 1994-C, pp. 165–174.

Aspler, L.B., Chiarenzelli, J.R., Bursey, T.L. 1993. Archean and Proterozoic geology of the Padlei belt, District of Keewatin, NWT, Geol. Surv. Can. Pap. 93-1C, pp. 147–158.

Aspler, L.B., Chiarenzelli, J.R., Ozarko, D.L., Powis, K.B. 1993. Geological map of the Watterson Lake area, District of Keewatin, NWT, Geol. Surv. Can. Open File 2767.

Aspler, L.B., Bursey, T.L., LeCheminant, A.N. 1992. Geology of the Henik, Montgomery Lake, and Hurwitz groups in the Bray-Montgomery-Ameto lakes area, southern District of Keewatin, Northwest Territories, Geol. Surv. Can. Pap. 92-1C, pp. 157–170.

Baragar, W.R.A., Scoates, R.F.J., 1987. Volcanic geochemistry of the northern segments of the Circum-Superior Belt of the Canadian Shield. In: Pharaoh, T.C., Beckinsale, R.D.,

Rickard, D. (Eds.), Geochemistry and Mineralization of Proterozoic Volcanic Suites, Geol. Soc. Lond. Spec. Publ. 33, pp. 113–131.

Baragar, W.R.A., Ernst, R.E., Hulbert, L., Peterson, T., 1996. Longitudinal petrochemical variation in the Mackenzie dyke swarm, northwestern Canadian Shield. J. Petrol. 37, 317–359.

Basaltic Volcanism Study Project, 1981. Basaltic Volcanism on the Terrestrial Planets, Pergamon Press, New York, 1286 pp.

Beavon, R.V., 1976. Early Aphebian basaltic volcanism in the southern District of Keewatin, Northwest Territories. Can. J. Earth Sci. 13, 1003–1005.

Bell, R.T., 1968. Preliminary notes on the Proterozoic Hurwitz Group, Tavani (55K) and Kaminak Lake (55L) areas, District of Keewatin, Geol. Surv. Can. Pap. 68-36, 17 pp.

Bell, R.T., 1970. Preliminary notes on the Hurwitz Group, Padlei map area, Northwest Territories, Geol. Surv. Can. Pap. 69-52, 13 pp.

Bridgwater, D., 1967. Feldspathic inclusions in the Gardar igneous rocks of South Greenland and their relevance to the formation of major anorthosites in the Canadian Shield. Can. J. Earth Sci. 4, 995–1014.

Buchan, K.L., Mortensen, J.K., Card, K.D., Percival, J.A., 1998. Paleomagnetism and U–Pb geochronology of diabase dyke swarms of Minto block, Superior Province, Quebec, Canada. Can. J. Earth Sci. 35, 1054–1069.

Buchan, K.L., Mertanen, S., Park, R.G., Pesonen, L.J., Elming, S.-Å., Abrahamsen, N., Bylund, G., 2000. Comparing the drift of Laurentia and Baltica in the Proterozoic: the importance of key paleomagnetic poles. Tectonophysics 319, 167–198.

Campbell, I.H., 2001. Identification of mantle plumes. In: Ernst, R.E., Buchan, K.L. (Eds.), Mantle Plumes: Their Identification Through Time, Geol. Soc. Amer. Spec. Pap. 352, pp. 5–21.

Canning, J.C., Henney, P., Morrison, M.A., Van Calsteren, P.W.C., Gaskarth, J.W., Swarbrick, A., 1998. The Great Glen Fault. A major vertical crustal boundary. J. Geol. Soc. Lond. 155, 425–428.

Chiarenzelli, J.R., Aspler, L.B., Villeneuve, M., Lewry, J.F., 1998. Paleoproterozoic evolution of the Saskatchewan Craton, Trans-Hudson Orogen. J. Geol. 106, 247–267.

Chevallier, L., Woodford, A., 1999. Morpho—tectonics and mechanism of emplacement of the dolerite rings and sills of the western Karoo, South Africa. South African J. Geol. 102, 43–54.

Condie, K.C., 2001. Mantle Plumes and their Record in Earth History. Cambridge University Press, Cambridge, p. 306.

Cousens, B.L., 1996. Magmatic evolution of Quaternary mafic magmas at Long Valley Caldera and the Devils Postpile, California: effects of crustal contamination on lithospheric mantle-derived magmas. J. Geophys. Res. 101, 27 673–27 689.

Cousens, B.L., Aspler, L.B., Chiarenzelli, J.R., Donaldson, J.A., Sandeman, H., Peterson, T.L., LeCheminant, A.N., 2001. Enriched Archean lithospheric mantle beneath Western Churchill Province tapped during Paleoproterozoic orogenesis. Geology 29, 827–830.

Davis, W.J., Aspler, L.B., Rainbird, R.H., Chiarenzelli, J.R. 2000. Detrital zircon geochronology of the Proterozoic Hurwitz and Kiyuk groups: a revised post-1.92 Ga age for deposition of the upper Hurwitz Group, GeoCanada 2000 Conference CD, Calgary.

DePaolo, D.J., Wasserburg, G.J., 1976. Nd isotopic variations and petrogenetic models. Geophys. Res. Lett. 3, 249–252.

Dupuy, C., Dostal, J., 1984. Trace element geochemistry of some continental tholeiites. Earth Planet. Sci. Lett. 67, 61–69.

Eade, K.E., 1973. Geology of Nueltin Lake and Edehon Lake (west half) map-areas, District of Keewatin, Geol. Surv. Can. Pap. 72-21, 29 pp.

Eade, K.E., 1974. Geology of Kognak River area, District of Keewatin, Northwest Territories, Geol. Surv. Can. Memoir 377, 66 pp.

Ellam, R.M., 1992. Lithospheric thickness as a control on basalt geochemistry. Geology 20, 153–156.

Elliot, D.H., Fleming, T.H., Kyle, P.R., Foland, K.A., 1999. Long-distance transport of magmas in the Jurassic Ferrar Large Igneous Province, Antarctica. Earth Planet. Sci. Lett. 167, 89–104.

Ernst, R.E., Buchan, K.L., 1993. Paleomagnetism of the Abitibi dyke swarm, southern Superior Province, and implications for the Logan Loop. Can. J. Earth Sci. 30, 1886–1897.

Ernst, R.E., Buchan, K.L., 1997. Giant radiating dyke swarms: their use in identifying pre-Mesozoic large igneous provinces and mantle plumes. In: Mahoney, J.J., Coffin, M.F. (Eds.), Large Igneous Provinces, American Geophys. Union Monogr. 100, pp. 297–333.

Ernst, R.E., Buchan, K.L., 1997. Layered mafic intrusions: a model for their feeder systems and relationship with giant dyke swarms and mantle plume centres. South African J. Geol. 100, 319–334.

Ernst, R.E., Buchan, K.L., 2001. The use of mafic dyke swarms in identifying and locating mantle plumes. In: Ernst, R.E., Buchan, K.L. (Eds.), Mantle Plumes: Their Identification Through Time, Geol. Soc. Amer. Spec. Pap. 352, pp. 247–265.

Ernst, R.E., Buchan, K.L., 2001. Large mafic magmatic events through time and links to mantle plume heads. In: Ernst, R.E., Buchan, K.L. (Eds.), Mantle Plumes: Their Identification Through Time, Geol. Soc. Amer. Spec. Pap. 352, pp. 483–575.

Ernst, R.E., Buchan, K.L., 2002. Maximum size and distribution in time and space of mantle plumes: evidence from large igneous provinces, J. Geodynamics 34, 309–432.

Ernst, R.E., Grosfils, E.B., Mège, D., 2001. Giant dike swarms: Earth, Venus and Mars. Annu. Rev. Earth Planet. Sci. 29, 489–534.

Fahrig, W.F., 1987. The tectonic settings of continental mafic dyke swarms: failed arm and early passive margin. In: Halls, H.C., Fahrig, W.F. (Eds.), Mafic Dyke Swarms, Geol. Assoc. Can. Spec. Pap. 34, pp. 331–348.

Fahrig, W.F., Christie, K.W., Eade, K.E., Tella, S., 1984. Paleomagnetism of the Tulemalu dykes, Northwest Territories, Canada. Can. J. Earth Sci. 21, 544–553.

Fedorenko, V.A., Lightfoot, P.C., Naldrett, A.J., Czamanske, G.K., Hawkesworth, C.J., Wooden, J.L., Ebel, D.S., 1996. Petrogenesis of the flood-basalt sequences at Noril'sk, north central Siberia. Int. Geol. Rev. 38, 99–135.

Fleming, T.H., Heimann, A., Foland, K.A., Elliot, D.H., 1997. 40Ar/39Ar geochronology of Ferrar Dolerite sills from the Transarctic Mountains, Antarctica: implications for the age and origin of the Ferrar magmatic province. Geol. Soc. Am. Bull. 109, 533–546.

Francis, E.H., 1982. Magma and sediment-I Emplacement mechanism of late Carboniferous tholeiite sills in northern Britain. J. Geol. Soc. Lond. 139, 1–20.

Fraser, J.A., 1983. Geology of Hyde Lake map area, District of Keewatin, N.W.T. Geol. Surv. Can. Pap. 82-9, 8 pp.

Gibbs, A.K., 1987. Contrasting styles of continental mafic intrusions in the Guiana Shield. In: Halls, H.C., Fahrig, W.F. (Eds.), Mafic Dyke Swarms. Geol. Assoc. Can. Spec. Pap. 34, pp. 457–466.

Goodwin, E.B., Thompson, G.A., Okaya, D.A., 1989. Seismic identification of basement reflectors: the Bagdad reflection sequence in the Basin and Range Province—Colorado Plateau transition zone, Arizona. Tectonics 8, 821–831.

Greenough, J.D., Hodych, J.P., 1990. Evidence for lateral magma injection in the Early Mesozoic dykes of eastern North America. In: Parker, A.J., Rickwood, P.C., Tucker, D.H. (Eds.), Mafic Dykes and Emplacement Mechanisms. Balkema, Rotterdam, pp. 35–46.

Griselin, M., Arndt, N.T., Baragar, W.R.A., 1997. Plume-lithosphere interaction and crustal contamination during formation of Coppermine River basalts, Northwest Territories, Canada. Can. J. Earth Sci. 34, 958–975.

Gvirtzman, Z., Garfunkel, Z., 1997. Vertical movements following intracontinental magmatism: an example from southern Israel. J. Geophys. Res. 102, 2645–2658.

Halls, H.C., Heaman, L.M., 2000. The paleomagnetic significance of new U–Pb age data from the Molson dyke swarm, Cauchon Lake area, Manitoba. Can. J. Earth Sci. 37, 957–966.

Hamilton, W., 1965. Diabase sheets of the Taylor Glacier region Victoria Land, Antarctica, U.S. Geol. Surv., Prof. Pap. 456-B, 71 pp.

Hansen, H., Grönvold, K., 2000. Plagioclase ultraphyric basalts in Iceland: the mush of the rift. J. Volc. Geoth. Res. 98, 1–32.

Hanmer, S., Aspler, L., Sandeman, H., Davis, W., Peterson, T., Relf, C., Ryan, J., Roest, W., 2000. Henik-Kaminak-Tavani supracrustal belt, late Archean oceanic crust and island arc remnants; upper crust protected from Proterozoic reworking, GeoCanada 2000 Conference CD, Calgary.

Hawkesworth, C.J., Gallagher, K., 1993. Mantle hotspots, plumes and regional tectonics as causes of intraplate magmatism. Terra Nova 5, 552–559.

Hawkesworth, C.J., Gallagher, K., Kirstein, L., Mantovani, M.S.M., Peate, D.W., Turner, S.P., 2000. Tectonic controls on magmatism associated with continental break-up: an example from the Paraná-Etendeka province. Earth Planet. Sci. Lett. 179, 335–349.

Heaman, L.M., 1994. 2.45 Ga global mafic magmatism: Earth's oldest superplume? In: Lauphere, M.A., Dalrymple, G.B., Turrin, B.D. (Eds.), Abstr. Eighth Int. Conf. on Geochron., Cosmochron. and Isotope Geol. U.S. Geol. Surv. Circ. 1107, 132.

Heaman, L.M., Corkery, M.T., 1996. U–Pb geochronology of the Split Lake block, Manitoba: preliminary results. In: Hajnal, Z., Lewry, J.F. (Eds.), Trans-Hudson Orogen Transect, Lithoprobe Report 55, pp. 60–68.

Heaman, L.M., LeCheminant, A.N., 1993. Paragenesis and U–Pb systematics of baddeleyite (ZrO_2). Chem. Geol. 110, 95–126.

Hemmingway, C.J., Sandeman, H.A., 1999. Geochemical and Sm–Nd isotopic study of Paleoproterozoic basaltic and gabbroic rocks of the Hurwitz Group, Kaminak Lake area, Kivalliq region, Northwest Territories, Geol. Surv. Can. 1999-F, pp. 53–62.

Heywood, W.W., 1973. Geology of Tavani map-area, District of Keewatin, Geol. Surv. Can. Pap. 72-47, 14 pp.

Hofmann, H.J., Davidson, A., 1998. Paleoproterozoic stromatolites, Hurwitz Group, Quartzite Lake area, Northwest Territories. Can. J. Earth Sci. 35, 280–289.

Hulbert, L., Williamson, B., Thériault, R., 1993. Geology of Middle Proterozoic MacKenzie diabase suites from Saskatchewan: an overview and their potential to host Noril'sk-type Ni–Cu–PGE mineralization. Sask, Geol. Surv. Misc. Rept. 93-3, pp. 112–126.

Hyndman, D.W., Alt, D., 1987. Radial dykes, laccoliths and gelatin models. J. Geol. 95, 763–774.

Lafrance, B., John, B.E., 2001. Sheeting and dyking emplacement of the Gunnison annular complex, SW Colorado. J. Struct. Geol. 23, 1141–1150.

Leaman, D.E., 1995. Mechanics of sill emplacement: comments based on the Tasmanian dolerites. Australian J. Earth Sci. 42, 151–155.

le Bas, M.J., le Maitre, R.W., Streckeisen, A., Zanettin, B., et al., 1986. A chemical classification of volcanic rocks based on the total alkali–silica diagram. J. Petrol. 27, 745–750.

Lucas, S.B., St-Onge, M.R., 1995. Syn-tectonic magmatism and development of compositional layering, Ungava Orogen (northern Quebec, Canada). J. Struct. Geol. 17, 475–491.

Mandler, H.A.F., Clowes, R.M., 1997. Evidence for extensive tabular intrusions in the Precambrian shield of western Canada: a 160-km-long sequence of bright reflections. Geology 25, 271–274.

McKenzie, D., McKenzie, J.M., Saunders, R.S., 1992. Dike emplacement on Venus and on Earth. J. Geophys. Res. 97, 15 977–15 990.

McPhie, J., 1993. The Tennant Creek porphyty revisited: a synsedimentary sill with peperite margins, Early Proterozoic, Northern Territory. Australian J. Earth Sci. 40, 545–558.

Mudge, M.R., 1968. Depth control of some concordant intrusions. Geol. Soc. Amer. Bull. 79, 315–332.

Naslund, H.R., McBirney, A.R., 1996. Mechanism of formation of igneous layering. In: Cawthorn, R.G. (Ed.), Layered Intrusions. Elsevier, Amsterdam, pp. 1–43.

Nykänen, V.M., Vuollo, J.I., Liipo, J.P., Piirainen, T.A., 1994. Transitional (2.1 Ga) Fe-tholeiitic-tholeiitic magmatism in the Fennoscandian Shield signifying lithospheric thinning during Paleoproterozoic extensional tectonics. Precambrian Res. 70, 45–65.

Parsons, T., Thompson, G.A., 1991. The role of magma overpressure in suppressing earthquakes and topography: worldwide examples. Science 253, 1399–1402.

Parsons, T., Sleep, N.H., Thompson, G.A., 1992. Host rock rheology controls on the emplacement of tabular intrusions: implications for underplating of extending crust. Tectonics 11, 1348–1356.

Patterson, J.G., 1991. The Spi Group: a post-Archean, pre-2.1 Ga rift succession, Trans-Hudson hinterland. Can. J. Earth Sci. 28, 1863–1872.

Patterson, J.G., Heaman, L.M., 1991. New geochronologic limits on the depositional age of the Hurwitz Group, Trans-Hudson hinterland, Canada. Geology 19, 1137–1140.

Peate, D.W., 1997. The Paraná-Etendeka Province. In: Mahoney, J.J., Coffin, M.F. (Eds.), Large Igneous Provinces, American Geophys. Union Monogr. 100, pp. 217–245.

Phinney, W.C., Halls, H.C., 2001. Petrogenesis of the Early Proterozoic Matachewan dyke swarm, Canada, and implications for magma emplacement and subsequent deformation. Can. J. Earth Sci. 38, 1541–1563.

Phinney, W.C., Morrison, D.A., Maczuga, D.E., 1988. Anorthosites and related megacrystic units in the evolution of Archean crust. J. Petrol. 29, 1283–1323.

Rubin, A.M., 1995. Propagation of magma-filled cracks. Annu. Rev. Earth Planet. Sci. 23, 287–336.

Sandeman, H., Cousens, B.L., Peterson, T., Hemmingway, C., Davis, W.J., Hanmer, S., Tella, S., 2000. Petrochemistry and Nd isotopic evolution of Proterozoic mafic rocks of the Western Churchill Province, Nunavut, and their implications for the evolution of the lithospheric mantle, GeoCanada 2000 Conference CD, Calgary.

Schledewitz, D.C.P., 1986. Geology of the Cochrane and Seal Rivers area, Manitoba Energy and Mines Geol. Rept. GR80-9, 139 pp.

Shaw, C.S.J., Young, G.M., Fedo, C.M., 1999. Sudbury-type breccias in the Huronian Gowganda Formation near Whitefish Falls, Ontario: products of diabase intrusion into incompletely consolidated sediments? Can. J. Earth Sci. 36, 1435–1448.

Stauffer, M.R., 1984. Manikewan: An Early Proterozoic ocean in central Canada, its igneous history and orogenic closure. Precambrian Res. 25, 257–281.

St-Onge, M.R., Scott, D.J., Lucas, S.B., 2000. Early partitioning of Quebec: Microcontinent formation in the Paleoproterozoic. Geology 28, 323–326.

Storey, B.C., 1995. The role of mantle plumes in continental breakup: case histories from Gondwanaland. Nature 377, 301–308.

Storey, B.C., Kyle, P.R., 1997. An active mantle mechanism for Gonwana breakup. South African J. Geol. 100, 283–290.

Sun, S.S., McDonough, W.F., 1989. Chemical and isotopic systematics of oceanic basalts; implications for mantle composition and processes. In: Saunders, A.D., Norry M.J. (Eds.), Magmatism in the Ocean Basins, Geol. Soc. London Sp. Pub. 42, pp. 313–345.

Symons, D.T.A., Gala, M., Palmer, H.C., 1995. Fitting paleomagnetic data to a plate tectonic model for the Trans-Hudson Orogen, with a focus on the Hanson Lake Block. In: Hajnal, Z., Lewrey, J. (Eds.), Trans-Hudson Orogen Transect Lithoprobe Report 48, pp. 66–77.

Tella, S., LeCheminant, A.N., Sanborn-Barrie, M.,Venance, K.E., 1997. Geology and structure of parts of MacQuoid Lake map area, District of Keewatin, Northwest Territories, Geol. Surv. Can. Pap. 1997-C, pp. 123–132.

Turner, S., Hawkesworth, C., Gallagher, K., Stewart, K., Peate, D., Mantovani, M., 1996. Mantle plumes, flood basalts, and thermal models for melt generation beneath continents: assessment of a conductive heating model and application to the Paraná. J. Geophys. Res. 101, 11 503–11 518.

Vigneresse, J.-L., Tikoff, B., Améglio, L., 1999. Modification of the regional stress field by magma intrusion and formation of tabular granitic plutons. Tectonophysics 302, 203–224.

Walker, G.P.L., 1999. Volcanic rift zones and their intrusion swarms. J. Volc. Geot. Res. 94, 21–34.

Weaver, B.L., 1991. The origin of ocean island basalt end-member compositions: trace element and isotopic constraints. Earth Planet. Sci. Lett. 104, 381–397.

White, R.S., 1992. Magmatism during and after continental break-up. In: Storey, B.C., Alabaster, T., Pankhurst, R.J. (Eds.), Magmatism and Causes of Continental Break-Up, Geol. Soc. Lond. Spec. Publ. 68, pp. 1–16.

White, R., McKenzie, D., 1995. Mantle plumes and flood basalts. J. Geophys. Res. 100, 17 543–17 585.

White, R., McKenzie, D., 1989. Magmatism at rift zones: the generation of volcanic continental margins and flood basalts. J. Geophys. Res. 94, 7685–7729.

Williams, H., Hoffman, P.F., Lewry, J.F., Monger, J.W.H., Rivers, T., 1991. Anatomy of North America: thematic portrayals of the continent. Tectonophysics 187, 117–134.

Wirth, K.R., Vervoort, J.D., 1995. Nd isotopic constraints on mantle and crustal contributions to Early Proterozoic dykes of the southern Superior Province. In: Baer, G., Heimann, A. (Eds.), Physics and Chemistry of Dykes. Balkema, Rotterdam, pp. 237–249.

Yeo, G.M., Delaney, G., Tran, H., 2000. Paleoproterozoic stratigraphy of the Wollaston Supergroup, Saskatchewan, GeoCanada 2000 Conference CD, Calgary.

Young, G.M., 1988. Proterozoic plate tectonics, glaciation and iron formations. Sediment. Geol. 58, 127–144.

Zhao, D., 2001. Seismic structure and origin of hotspots and mantle plumes. Earth Planet. Sci. Lett. 192, 251–265.